Experimental and computational studies of the stability and reactivity of a half-sandwich 16-electron spin triplet Mo^{II} complex containing a terminal hydroxide ligand†

Rinaldo Poli*[a] and Elsje Alessandra Quadrelli[b]

[a] *Laboratoire de Synthèse et d'Electrosynthèse Organometallique, Faculté des Sciences "Gabriel", Université de Bourgogne, 6 Boulevard Gabriel, 21100 Dijon, France*
[b] *Department of Chemistry and Biochemistry, University of Maryland, College Park, MD 20742, USA*

Compound $CpMo(OH)(PMe_3)_2$, **1**, a stable monomeric 16-electron organometallic complex with a spin triplet ground state and a terminal hydroxide ligand, is obtained from the reaction of $CpMoCl(PMe_3)_3$ with KOH. Density functional (B3LYP) geometry optimizations for a $CpMo(OH)(PH_3)_2$ model system afford a spin triplet ground state with a bent *endo* hydroxide ligand. An excited singlet state with a bent *exo* OH ligand is found 2.27 kcal mol^{-1} higher in energy. Analogous calculations on other related $CpMoX(PH_3)_2$ systems provide a spin triplet ground state for X = Cl and H, whereas the compound with X = PH_2 has a singlet ground state. Addition of PH_3 leads to a calculated bond energy of 20.9, 14.3, 7.2 and 6.8 kcal mol^{-1} relative to the 16-electron singlet state for H, Cl, PH_2 and OH, respectively. These values are consistent with qualitative expectations based on the strength of the Mo—X π interaction and steric strain in the $CpMo(PH_3)_3$ and $CpMo(PH_3)_2$ fragments. Crude estimates of the thermodynamic strength of the Mo—X π interactions have been derived. The calculations also show that an α-H elimination from the hydroxide ligand to afford $CpMoH(O)(PH_3)$ plus PH_3 should be thermodynamically favored but suggest that it is kinetically difficult. Compound **1** slowly decomposes in C_6D_6 in the presence of PMe_3 by a process that is initiated by the activation of a solvent C—D bond. This process produces a mixture of $CpMoH(PMe_3)_3$, **4**, $CpMo(\eta^2\text{-}CH_2PMe_2)(PMe_3)_2$, **5**, C_6D_5OH and PMe_3-d^n (n = 1–9) molecules. The relative isotopic distribution of the free PMe_3-d^n molecules can be satisfactorily simulated. The analogous decomposition of $CpMo(OD)(PMe_3)_2$ (**1**-OD) revealed a rapid exchange of the deuteroxide D atom and a PMe_3 ligand H atom. The decomposition of **1** in the presence of PMe_3 in C_6D_6 is catalyzed by water or methanol. The molecules are believed to engage in hydrogen bonding interactions with the OH lone pairs, thereby modifying the electronic structure of compound **1** and enhancing the reactivity toward the oxidative addition of the solvent C—D bonds.

Understanding the relationship between structure (both molecular and electronic) and reactivity has always constituted a challenge for chemistry in general and organometallic chemistry in particular. The relevance of such factors as orbital overlap, π filled-filled repulsion,[1] push-pull interactions[1] and ligand–ligand repulsive (steric) effects,[2,3] are commonly discussed. The influence of the spin state on the structure, stability and reactivity is appreciated for Werner-type coordination compounds, but application to organometallic chemistry has been neglected due to the relative paucity of high-spin compounds.[4] Some of our recent contributions have been directed toward filling this gap. In particular, we have shown by both experimental and theoretical studies that an unsaturated intermediate may be energetically stabilized by the release of pairing energy by adopting a higher spin state,[5–15] with the immediate effect of weakening metal–ligand interactions and accelerating ligand dissociation processes for more saturated, lower spin state compounds.

A particular system of interest is the 16-electron $CpMoXL_2$, where X is a one-electron ligand and L a two-electron ligand, according to the Green classification.[16] While most combinations of X and L give extremely reactive, short-lived intermediates, a few stable and diamagnetic examples containing strongly π-donating X groups (*e.g.*, phosphido, arsenido) have been described.[17–19] We have recently reported the first examples of this class having a spin triplet ground state, *i.e.* complexes Cp^*MoClL_2(L = PMe_3, PMe_2Ph; L_2 = dppe),[20,21] and studied the influence of the spin state change on the kinetics of the ligand addition to afford 18-electron diamagnetic adducts.[12] We have proposed that the relative stability of these compounds toward ligand addition or oxidative addition processes can be attributed in part to the release of pairing energy by adopting the spin triplet ground state, alongside the steric protection offered by the bulky Cp* ligand. The importance of steric factors is shown by the equilibrium favoring the 16-electron species for PMe_3 addition to $Cp^*MoCl(PMe_3)_2$, whereas compound $CpMoCl(PMe_3)_3$ does not dissociate PMe_3 to any measurable extent.[21] Theoretical MP2 calculations estimated a 10.9 kcal mol^{-1} stabilization of triplet $CpMoCl(PH_3)_2$ relative to the corresponding singlet.[12]

An important question is whether steric protection is always necessary in order to stabilize this class of compounds. We thus turned our attention to less bulky Cp derivatives containing the hydroxide ligand. This ligand can be foreseen to provide additional stability to an unsaturated system by virtue of both its expected greater π-donating power and the possibility of providing greater pairing energies, *i.e.* greater energetic stabilization for the triplet state, because of a greater electronegativity of the oxygen atom. Our investigations, which are reported here, have allowed us not only to prepare

† Dedicated to Roald Hoffmann in recognition of the influence of his teaching on our thinking.
Non-SI units employed: cal ≈ 4.18 J; hartree ≈ 2.63 × 10^6 J mol^{-1}.

the desired hydroxo complex, but also to gather useful experimental and theoretical information on the relationship between the molecular and electronic structures and the reactivity. A preliminary account of part of this work has appeared.[22]

Experimental

General

All operations were carried out under an atmosphere of dinitrogen with standard Schlenk-line techniques. Solvents were purified by conventional methods and distilled under argon prior to use (THF and Et_2O from Na–benzophenone, heptane from Na, acetone from $CaSO_4$). Deuterated solvents (C_6D_6, C_6D_{12} and CD_3COCD_3) were degassed by three freeze-pump-thaw cycles and then stored over 4 Å molecular sieves under dinitrogen. NMR spectra were obtained with Bruker WP200 and AF200 spectrometers. The peak positions are reported with positive shifts downfield of TMS as calculated from the residual solvent peaks (^1H) or downfield of external 85% H_3PO_4 (^{31}P). For each ^{31}P NMR spectrum, a sealed capillary containing H_3PO_4 was immersed in the same NMR solvent used for the measurement and this was used as reference. FT-IR spectra were recorded on a Perkin-Elmer 1880 spectrometer with KBr cells. GC-MS spectra were obtained on a GC-17a/QP-5000 Schimadzu analyzer, equipped with a Perkin Elmer column type DB5 (5% diphenyl–95% dimethyl polysiloxane). $CpMoCl(PMe_3)_3$ and $CpMoH(PMe_3)_3$ were prepared as previously published.[23] KOH and NaOD were purchased from Aldrich and dried at 110 °C, 6 mm Hg for 56 h. Cp_2FeBF_4, PMe_3-d^9 and $LiEt_3BD$ in THF (Aldrich) were used as received.

Syntheses and reactions

Preparation of $CpMo(OH)(PMe_3)_2$, 1. Solid KOH (*ca.* 300 mg, *ca.* 5.3 mmol) was added to a blue solution of $CpMoCl(PMe_3)_3$ (215 mg, 0.507 mmol) in 6 mL of THF. After stirring overnight at room temperature, complete evaporation of the solvent from the yellow-brown solution yielded an oily residue, which was extracted into heptane (3 × 5 mL). The leftover white precipitate was filtered off and dried, and subsequently redissolved in water, giving a positive Ag^+/HNO_3 test for Cl^- ions. An aliquot of the yellow-brown heptane solution was dried under reduced pressure and the residue was investigated by ^1H NMR and IR in C_6D_6. ^1H NMR (C_6D_6, δ): 21.8 (br, 18H, $w_{1/2} = 90$ Hz, Me), 20.3 (br, 5H, $w_{1/2} = 75$ Hz, Cp). IR (C_6D_6, cm^{-1}): 3092(w), 2960(s), 2897(s), 2801(w), 2280(s), 2266(s), 1785(m), 1750(m), 1419(s), 1270(s), 1101(m), 930(s), 820(m). The mother liquor, concentrated to 1 mL, did not separate a solid even at −80 °C.

An analogous reaction was carried out in C_6D_6 and monitored by ^1H NMR, showing the concomitant formation of **1** and one equivalent of free PMe_3. ^1H NMR (C_6D_6, δ): 0.791 (d, $J_{PH} = 2.9$ Hz). $^{31}P\{^1H\}$ NMR (C_6D_6, δ): −61.8 (s). Continued ^1H NMR monitoring of this solution showed a slow decrease in the intensity of the resonances of **1** and the growth of new resonances attributed to $CpMoH(PMe_3)_3$, **4**, and $CpMo(PMe_3)_2(\eta^2\text{-}CH_2PMe_2)$, **5**, by comparison with the literature spectra.[23] Compound **4**: ^1H NMR (C_6D_6, δ): 4.48 (s, 5H, Cp), 1.29 (vt, $J_{HP} = 9$ Hz, 27H, PMe_3), −8.35 (q, $J_{HP} = 53$ Hz, 1H, H). $^{31}P\{^1H\}$ NMR (C_6D_6, δ): 21.7 (s, PMe_3). Compound **5**: ^1H NMR (C_6D_6, δ): 4.32 (s, 5H, Cp), 1.25 (d, $J_{HP} =$ 9 Hz, 6H, PMe_2), 1.2 (br), −0.38 (br, 2H, CH_2). $^{31}P\{^1H\}$ NMR (C_6D_6, δ): 26.9 (d, 2P, PMe_3, $J_{PP} = 40$ Hz), −40.6 (t, 1P, PMe_2CH_2, $J_{PP} = 40$ Hz). The ratio of **4** and **5** is *ca.* 4 : 1 from ^1H NMR integration. *Ca.* 70% decomposition had occurred after 10 days at room temperature.

Thermal stability of 1. Compound **1** (45 mg, 0.11 mmol) was dissolved in C_6D_6 in an NMR tube, which was then flame-sealed. No change in the ^1H NMR properties was observed upon warming to 70 °C over a period of two hours, except for the expected temperature shift of the contact-shifted resonances of **1** (see *Results*). Upon further warming to 95 °C for 18 h, the resonances of **1** disappeared and were not replaced by any new resonance attributable to diamagnetic Cp-containing compounds.

Preparation of $CpMo(OD)(PMe_3)_2$, 1-OD. Solid NaOD was added to a solution of $CpMoCl(PMe_3)_3$ (40 mg, 0.09 mmol) in C_6D_6 (1 mL) and left to stir overnight. An aliquot was taken for the NMR analysis. The formation of compound $CpMo(OD)(PMe_3)_2$, **1**-OD, and free PMe_3 was indicated by the ^1H resonances at δ 21.8 and 20.3 for the former, and by the ^1H resonance at δ 0.79 and the ^{31}P resonance at δ −61.9 for the latter. The remaining solution was used for an IR investigation. IR (C_6D_6, cm^{-1}): 2959(s), 2895(s), 2638(m), 2388(w), 2280(s), 2266(s), 1617(m), 1332(s), 1261(s), 1101(m), 924(s), 817(m).

Reaction of 1 with CO. Solid KOH (*ca.* 10 mg) was added to a blue solution of $CpMoCl(PMe_3)_3$ (30 mg, 0.07 mmol) in THF (2 mL) and the suspension was left to stir overnight. The yellow-brown mother liquor was filtered into a new Schlenk tube and evaporated to dryness; the residue was dissolved in C_6D_6. An aliquot of the resulting solution was investigated by ^1H NMR, confirming the presence of **1**. The atmosphere in the reaction vessel was changed to CO; an immediate color change from brown to red ensued. An aliquot of the solution was investigated by ^1H NMR spectroscopy, showing the complete disappearance of the resonances of **1**. A complex mixture of diamagnetic Cp-containing non-hydridic complexes had formed. A major product, whose intensity accounted for more than 50% of the peaks, was identifiable. ^1H NMR: (C_6D_6, δ): 4.74 (s, Cp), 1.28 (m, Me). A second aliquot was investigated by IR spectroscopy in the CO-stretching vibration region. IR (KBr, 2000–1700 cm^{-1}): 1933(s), 1891(w), 1849(vs), 1780(s).

Ferrocenium oxidation of 1 in the presence of PMe_3. A solution containing equimolar amounts of **1** and PMe_3 was prepared *in situ* as described above by reacting $CpMoCl(PMe_3)_3$ (222 mg, 0.522 mmol) and an excess of dry KOH for 8 h in THF (10 mL), followed by filtration through Celite. To the resulting solution was added dropwise a solution of Cp_2FeBF_4 (140 mg, 0.512 mmol) in THF (20 mL). The solution was evaporated to dryness at reduced pressure and the residue was washed with diethyl ether until the washings were colorless (3 × 10 mL). The light-orange solid was dried under vacuum and recovered as a powder (99 mg). Crystals suitable for an X-ray analysis {yellow needles of $[CpMo(OH)(PMe_3)_3]BF_4$, **2**, and red prisms of $[CpMo(O)(PMe_3)_2]BF_4$, **3**} were obtained from an acetone solution upon slow diffusion of a heptane layer. A unit cell determination confirmed the nature of the yellow needles as **2** by comparison with the literature,[22] while a ^1H and ^{31}P NMR investigation of the red prisms confirmed their identity as **3**, by comparison with the values previously reported.[22,24] The relative amount of products **2** and **3** could not be established, as compound **2** is NMR-silent.

NMR monitoring of the reaction of 1 and PMe_3 in C_6D_6. A solution of **1** and PMe_3 was prepared by stirring dry KOH (*ca.* 70 mg) and $CpMoCl(PMe_3)_3$ (84 mg, 0.198 mmol) in C_6D_6 (3 mL). After 18 h, an aliquot of the brown suspension

(*ca.* 0.5 mL) was transferred to an NMR tube and the tube was flame-sealed. The ^1H and ^{31}P NMR spectra show the resonances of **1**, **4**, **5** and unidentified Cp-containing by-products in an approximate 75 : 18 : 5 : 2 ratio. The evolution of these spectra is described in the *Results* section. They revealed the formation, *inter alia*, of PMe_3-d^n. In the ^{31}P NMR spectrum each isotopomer generates a singlet shifted upfield with respect to free PMe_3. The shift is proportional to the deuterium content and consists in 0.305 ppm per deuterium atom. The ppm separation between peaks is constant upon change in the spectrometer magnet strength.

NMR monitoring of the reaction of 1-OD and PMe_3 in C_6D_6. $CpMoCl(PMe_3)_3$ (100 mg, 0.235 mmol) and an excess of dry NaOD were introduced in an NMR tube containing C_6D_6 (0.5 mL). The tube was flame-sealed and the reaction was monitored by ^1H and ^{31}P NMR spectrometry. The formation of compound $CpMo(OD)(PMe_3)_2$, **1**-OD, and free PMe_3 was confirmed by ^1H and ^{31}P NMR (*vide supra*). The evolution of this spectrum is analogous to that of the experiment described in the previous paragraph, with a notable exception for the resonance of PMe_3-d^1 (see *Results*).

NMR monitoring of the reaction of 1 and PMe_3 in C_6D_{12}. A solution of **1** in C_6D_{12} (*ca.* 0.2 mmol in 0.5 mL) was transferred to an NMR tube and Cp_2Fe added as an internal standard (21 mg, 0.112 mmol). The tube was sealed and the reaction monitored over time. ^1H NMR (C_6D_{12}, δ): 22.2 (br, 18H, $w_{1/2}$ = 80 Hz, Me), 20.8 (br, 5H, $w_{1/2}$ = 65 Hz, Cp). Free PMe_3 is also present, residual from the synthesis of **1**. After a few days there is no noticeable change. After one month, more than 50% of **1** is still in solution and some red precipitate has separated. Resonances attributed to **5** are present. Their intensity accounts for 50% of the decomposed starting material. No activation of free PMe_3 is noticed.

NMR monitoring of the reaction of 1 and PMe_3-d^9 in C_6D_6. Compound **1** was prepared *in situ* as described above from $CpMoCl(PMe_3)_3$ (200 mg, 0.470 mmol) and dry NaOH in C_6D_6 (2 mL). An aliquot (1 mL) was transferred to an NMR tube and evaporated to dryness under vacuum to remove the free phosphine. To the residue was added C_6D_6 (0.5 mL) and PMe_3-d^9 (0.1 mL, 9.7 mmol). The reaction was monitored by ^1H and ^{31}P NMR spectrometry (see *Results*).

Addition of a Brønsted acid to the reaction of 1 and PMe_3 in C_6D_6. (*a*) *Water*. A solution of **1** was prepared *in situ* as described above from $CpMoCl(PMe_3)_3$ (46 mg, 0.11 mmol) and an excess of dry KOH in C_6D_6 (1 mL). The yellow-brown supernatant was split into two equal parts, which were transferred to two NMR tubes. H_2O (5 μL) was added to one of the tubes and then both were monitored by ^1H and ^{31}P NMR spectrometry. While **1** had undergone <5% transformation in the water-free tube after 48 h, the water-containing tube showed the complete replacement of the resonances of **1** with those of **4** and **5** (**4** : **5** ratio = 10 : 1). No other Cp-containing products were observed. An aliquot of the water-containing sample was diluted in air with *ca.* 50 parts of CH_2Cl_2, and an aliquot of the resulting solution was subsequently analyzed by GC-MS (50–300 °C, 17° min^{-1}; EI, scan *m/z* 50–500). C_6D_5OH was identified as a by-product (retention time = 5.79 ± 0.04 min, M^+ = 99) by comparison with a genuine sample of C_6H_5OH under the same conditions (retention time = 5.77 ± 0.04 min, M^+ = 94).

(*b*) *Methanol*. A solution of **1** was prepared *in situ* as described above from $CpMoCl(PMe_3)_3$ (84 mg, 0.198 mmol) and an excess of dry KOH in C_6D_6 (1 mL). The yellow-brown supernatant was split into two equal parts, which were transferred into two NMR tubes. MeOH (10 μL) was added to one of the tubes and then both were monitored by ^1H and ^{31}P NMR spectrometry. **1** was completely consumed within 2 h in the MeOH-containing tube (**4** : **5** ratio = 10 : 1), while it was still present after 24 h in the other tube (**4** : **5** ratio = 4 : 1). No other Cp-containing products were observed.

Oxidation of 1 and PMe_3 in C_6D_6. A solution of ferrocenium (Fc^+) hexafluorophosphate (8.8 mg, 26 μmol) in acetone-d^6 (0.70 mL, 38 mM) was prepared. A solution of **1** was prepared *in situ* as described above by reacting $CpMoCl(PMe_3)_3$ (142 mg, 0.334 mmol) and an excess of dry KOH for 8 h in C_6D_6 (0.9 mL, 0.37 M). An aliquot of the yellow-brown supernatant (0.35 mL, 0.130 mmol) was transferred to an NMR tube containing neat acetone-d^6 (0.30 mL), and a second aliquot was transferred to an NMR tube containing the ferrocenium solution (0.30 mL, 11 μmol, Fc^+/Mo = 0.08). NMR monitoring showed no significant difference between the two reactions after 48 h.

NMR monitoring of the reaction of 4 and PMe_3-d^9 in C_6D_6. To a solution of **4** (0.03 mmol) in C_6D_6 (0.5 mL) containing free PMe_3-d^0 (0.1 mmol), PMe_3-d^9 was added in threefold excess. The PMe_3-d^0 : PMe_3-d^9 ratio increased within hours and complete equilibration was reached in three days (equilibrium ratio = *ca.* 1 : 1 from ^{31}P NMR). No PMe_3-d^n ($1 \leqslant n \leqslant 8$) was detected.

Reaction of $CpMoCl(PMe_3)_3$ with CO. A toluene solution (5 mL) of $CpMoCl(PMe_3)_3$ (30 mg, 70 μmol) was exposed to an atmosphere of CO; the blue solution immediately turned yellow. An aliquot of the solution was transferred into another Schlenk tube and evaporated to dryness, followed by redissolution of the residue in C_6D_6. The observed resonances at δ 4.67 (s, Cp) and 1.30 (d, PMe_3, J_{HP} = 9 Hz) in the ^1H NMR and at δ 21.0 in the ^{31}P NMR spectra, and the CO stretching frequency at 1789 cm^{-1} in the IR spectrum, are assigned to $CpMoCl(CO)(PMe_3)_2$ by comparison with the literature values.[25]

Reaction of $CpMoCl(PMe_3)_3$ with $LiEt_3BD$ in THF-d^8. A 1 M solution of $LiEt_3BD$ in THF (68 μL, 68 μmol) was evaporated to dryness under vacuum and the residue was dissolved in THF-d^8 (0.5 mL). Solid $CpMoCl(PMe_3)_3$ (27 mg, 64 μmol) was added and the solution was stirred for 1 h at room temperature. The solution was then transferred to an NMR tube for a ^1H NMR investigation. The spectrum showed the expected resonances for **4**, including the hydridic P-coupled quartet at −8.35 ppm (J_{HP} = 53 Hz) with an approximately correct intensity relative to the Cp resonance (*ca.* 1 : 5).

Theoretical calculations

All electronic structure and geometry optimization calculations were performed using GAUSSIAN 94[26] on the SGI Power Challenge at the Université de Bourgogne. The LanL2DZ set was employed to perform complete geometry optimization with a density functional theory (DFT) approach. The three-parameter form of the Becke, Lee, Yang and Parr functional (B3LYP)[27] was employed. The LanL2DZ basis set includes both Dunning and Hay's[28] D95 sets for H

and C and the relativistic electron core potential (ECP) sets of Hay and Wadt for the heavy atoms.[29–31] Electrons outside the core were all those of the H, C and O atoms, the 3s, 3p electrons in Cl and P, and the 4s, 4p, 4d and 5s electrons in Mo. A C_s symmetry arrangement was imposed for the $CpMoX(PH_3)_n$ systems (X = OH, Cl, H, PH_2; $n = 2$, 3) and for the *trans*-$CpMoH(O)(PH_3)_2$ system. No constraints were imposed for the C_1-symmetric systems.

The mean value of the spin of the first-order electronic wavefunction, which is not an exact eigenstate of S^2 for unrestricted calculations on open-shell systems, was considered suitable to identify the spin state unambiguously. Spin contamination was carefully monitored and the energies shown in the *Results* section correspond to unrestricted B3LYP (UB3LYP) calculations. The value of $\langle S^2 \rangle$ for the UB3LYP calculations on open-shell systems at convergence were: $CpMo(OH)(PH_3)_2$, 2.0123; $CpMoCl(PH_3)_2$, 2.0128; $CpMoH(PH_3)_2$, 2.0138; $CpMo(PH_2)(PH_3)_2$, 2.0143; *trans*-$CpMoH(O)(PH_3)_2$, 2.0167 and *cis*-$CpMoH(O)(PH_3)_2$, 2.0134 for the spin triplet systems; $CpMo(PH_3)_3$, 0.7556 and $CpMo(PH_3)_2$, 0.7558 for the spin doublet systems, indicating minor spin contamination.

Results

(*A*) Synthesis and characterization of $CpMo(OH)(PMe_3)_2$, 1

$CpMoCl(PMe_3)_3$ reacts with dry KOH in THF or C_6D_6 to yield insoluble KCl and $CpMo(OH)(PMe_3)_2$, **1**, along with free trimethylphosphine (see eq. 1). If the KOH is not dry, the reaction products rapidly engage in a decomposition reaction, which is discussed in detail in section (*C*) below. NMR monitoring of the reaction in C_6D_6 allowed us to observe directly the formation of one equivalent of PMe_3 concomitantly with **1**. The reaction is selective, no other products being detected by ^1H NMR spectroscopy under dry conditions (see Fig. 1 of ref. 22).

$$CpMoCl(PMe_3)_3 + KOH \rightarrow CpMo(OH)(PMe_3)_2 + KCl + PMe_3 \quad (1)$$

1

Compound **1** is extremely soluble in all common organic solvents, including saturated hydrocarbons at −80 °C and $Me_3SiOSiMe_3$. The ^1H NMR spectrum of **1** in C_6D_6 displays two paramagnetically shifted resonances at 21.8 and 20.3 ppm in a 18 : 5 ratio. These resonances shift linearly with the inverse temperature in the 30–75 °C temperature range (see Fig. 1), as expected for a Curie paramagnet. The OH resonance could not be observed in the ^1H NMR spectrum. Warming to a higher temperature for an extended period of time resulted in complete decomposition of **1** to give a mixture

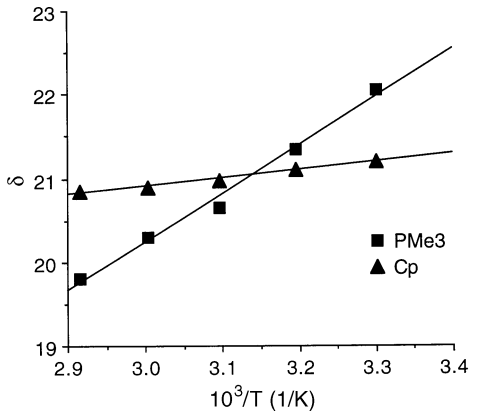

Fig. 1 Temperature dependence of the contact-shifted resonances for compound **1**. Solvent = C_6D_6

of Cp complexes that we have not further investigated. The IR spectrum of **1** shows a weak absorbance at 3092 cm^{-1} in C_6D_6, assigned to the OH stretching vibration. This band is replaced by a vibration at 2388 cm^{-1} for the deuterated analogue $CpMo(OD)(PMe_3)_2$ [**1**-OD], which was synthesized according to eq. 1 by using anhydrous NaOD.

As implied by the synthetic procedure, **1** does not bind PMe_3 nor N_2. Neither is any transformation observed upon exposure to an atmosphere of H_2. On the other hand, the isoelectronic complex $Cp^*MoCl(PMe_3)_2$ reacts with all the above molecules to afford ligand addition (PMe_3, N_2) and oxidative addition (H_2) products.[20,21] Like the chloro complex, however, **1** reacts with CO, yielding a mixture of diamagnetic products as shown by the complexity of the ^1H NMR and IR spectra (see *Experimental*). We assume that this reaction is initiated by addition of CO to **1** to generate the 18-electron compound $CpMo(OH)(PMe_3)_2(CO)$, followed by subsequent transformations that we have not further investigated.

Compound **1** is formulated as a monomeric species with a spin triplet ground state. The alternative formulation as a bis(hydroxo)-bridged dimer is excluded because it would involve electronically saturated (18-electron) metal centers, leading to diamagnetism. Electronically saturated organometallic complexes have never been found to be paramagnetic for transition metals beyond the 3d series, and there are arguments against the occupation of metal-ligand antibonding orbitals for such complexes.[4] An example of a diamagnetic, dinuclear compound with the same stoichiometry as **1** is $[CpMo(\mu\text{-}Br)(\eta^4\text{-}C_4H_6)]_2$.[32] The contact shifts observed for the ^1H NMR resonances of Cp and phosphine α-H atoms in **1** are comparable with those reported for other 16-electron half-sandwich Mo^{II} complexes, namely Cp^*MoClL_2 (L = PMe_3, PMe_2Ph or L_2 = dppe) and $CpMoCl(PMe_2Ph)_2$.[21] A possible alternative formulation as an oxo-hydrido Mo^{IV} derivative, $CpMoH(O)(PMe_3)_2$, is not consistent with the IR data. In addition, such a formulation should lead to a diamagnetic ground state by virtue of its 18-electron configuration. The computational work [see section (*F*) below] further supports this conclusion.

(*B*) Oxidation of 1 in the presence of PMe_3

As compound **1** could not be crystallized and analyzed, its formulation has been further confirmed by a derivatization study. Treatment of an equimolar solution of **1** and PMe_3, formed *in situ* from the parent chloride according to eq. 1, with one equivalent of $Cp_2Fe^+BF_4^-$ leads to a red solution from which yellow needles of $[CpMo(OH)(PMe_3)_3]^+BF_4^-$, **2**, and red cubes of $[CpMoO(PMe_3)_2]^+BF_4^-$, **3**, have been isolated (see eqs. 2 and 3). The presence of a terminal hydroxo ligand in compound **2** was previously confirmed by X-ray crystallography, including the direct location of the hydroxide H atom.[22] The stoichiometry of eq. 3 requires the formation of protons, which are probably trapped by the phosphine ligand that is concomitantly liberated by the reaction. Further studies of this oxidation process will be reported elsewhere.[33]

$$CpMo(OH)(PMe_3)_2 + PMe_3 + Fc^+ \rightarrow [CpMo(OH)(PMe_3)_3]^+ + Fc \quad (2)$$

$$[CpMo(OH)(PMe_3)_3]^+ + Fc^+ \rightarrow [CpMo(O)(PMe_3)_2]^+ + PHMe_3^+ + Fc \quad (3)$$

(*C*) Decomposition of 1 in C_6D_6

C_6D_6 solutions of **1**–PMe_3 slowly decompose (75% in 30 days) upon standing at room temperature in a sealed NMR tube, to afford the previously reported[23] complexes $CpMoH(PMe_3)_3$, **4**, and $CpMo(\eta^2\text{-}CH_2PMe_2)(PMe_3)_2$, **5**, as

main products in a *ca.* 4 : 1 ratio. The rate of this decomposition is highly dependent on the solvent, the relative rate of transformation being C_6D_6 > THF > C_6D_{12}. The stability in THF was checked by periodically withdrawing aliquots of the solution and recording the NMR spectra in acetone-d^6. After 5 days, 30% decomposition is seen in C_6D_6, while only traces of **4** are seen in THF and none in C_6D_{12}. While the compound leads to observable amounts of **5** (*but no 4!!!*) in C_6D_{12} after 10 days, its THF solutions are unstable over long periods of time and lead to insoluble powders, which were not further investigated.

A more detailed study in C_6D_6 with ^1H and ^{31}P NMR monitoring shows the formation of C_6D_5H and deuterated PMe_3. All possible PMe_3-d^n ($n = 1$–9) isotopomers are obtained, with the isotopic distribution favoring the fully deuterated product since the initial stages [see Fig. 2(*a*)]. The isotopic distribution changes over time, with the heaviest phosphines becoming even more prevalent. The appearance of free PMe_3-d^n occurs on a longer time scale relative to the disappearance of **1** and the appearance of C_6D_5H. This is due to the slow release of the deuterated ligand from the coordination sphere in complex **4** (see *Discussion*). On the other hand, no D incorporation into free PMe_3 is observed when the experiment is carried out in C_6D_{12}. In addition, the NMR studies show that the presence of water or methanol greatly increases the decomposition rate (only a few hours at room temperature for the complete disappearance of **1** and PMe_3). The nature of all the decomposition products remains unchanged, but the **4** : **5** ratio is significantly greater in the presence of these catalysts (*ca.* 10 : 1). A GC-MS investigation of the solution resulting from the water-catalyzed decomposition also reveals the presence of pentadeuterophenol, C_6D_5OH. The addition of ferrocenium does not affect the decomposition rate, ruling out the intervention of an electron-transfer-catalysis (ETC) mechanism.[34] As shown in the previous section, ferrocenium is a sufficiently strong oxidizing agent to oxidize **1** in the presence of PMe_3. Carrying out the decomposition reaction under H_2 also has no effect on the rate and the nature of the products.

In order to establish whether the hydrido ligand in product **4** originates from the hydroxo proton of **1**, an analogous study was carried out on the deuteroxo complex **1**-OD. From the integration of a ^1H NMR spectrum, the majority of product **4** that is obtained during the initial stages of this experiment (< 10% decomposition) contains a *hydrido* ligand. A $^{31}P\{^1H\}$ NMR experiment shows that the main resonance for **4** is a singlet. Flanking resonances that could be assigned to a 1 : 1 : 1 triplet for **4**-D are estimated as < 30% of the total intensity. This and all the other results are identical with those of the decomposition of **1**, except for a higher relative proportion of the PMe_3-d^1 product of H/D exchange [see Fig. 1(*b*)].

(*D*) Phosphine-exchange studies for 1 and 4

In order to find supporting evidence for the overall proposed mechanism of the decomposition of **1** and H/D exchange between PMe_3 and C_6D_6 (see *Discussion*), we have independently investigated the PMe_3 exchange process for both **1** and **4**. ^1H and ^{31}P monitoring of the reaction between **1**-d^0 and PMe_3-d^9 in C_6D_6 (eq. 4) shows the rapid growth of the resonances attributable to free PMe_3-d^0. The half-life of this process is approximately 8 h at room temperature under the conditions described in the *Experimental* section. This experiment also shows the small but significant growth of a ^{31}P resonance due to free PMe_3-d^8 ($d^0 : d^8 : d^9$ *ca.* 10 : 1 : 100 after 35 min at ambient temperature). No other PMe_3-d^n isotopomers are formed in observable amounts during this process.

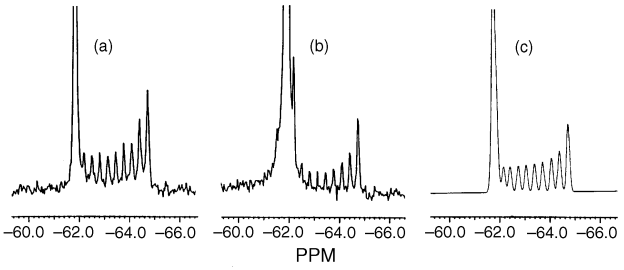

Fig. 2 ^{31}P NMR spectra in the resonance region of free PMe_3 for the **1** + PMe_3 + C_6D_6 reaction at room temperature. (*a*) Reaction of compound **1**; $t = 120$ days. (*b*) Reaction of **1**-OD; $t = 90$ days. (*c*) Simulation of the experimental isotopic distribution shown in (*a*)

$$CpMo(OH)[P(CH_3)_3]_2 + 2P(CD_3)_3 \rightarrow CpMo(OH)[P(CD_3)_3]_2 + 2P(CH_3) \quad (4)$$

An exchange of PMe_3 also occurs for **4**, as shown by the analogous ^1H and ^{31}P monitoring of the **4**-d^0/PMe_3-d^9 reaction (eq. 5). This reaction, however, is slower with respect to the corresponding exchange on compound **1** (half-life *ca.* 1 day with a threefold excess of PMe_3-d^9), and no free PMe_3 isotopomers other than PMe_3-d^0 are observable in the ^{31}P NMR spectrum.

$$CpMoH[P(CH_3)_3]_3 + 3P(CD_3)_3 \rightarrow CpMoH[P(CD_3)_3]_3 + 3P(CH_3)_3 \quad (5)$$

(*E*) Attempted synthesis of 4-D

Since $CpMoD(PMe_3)_3$ (**4**-D) is a possible product of the decomposition of **1** in C_6D_6 (see *Discussion*), we have attempted to synthesize it by adapting the synthetic strategy previously employed for the synthesis of **4**, namely the metathesis reaction of the chloride precursor $CpMoCl(PMe_3)_3$ with $LiEt_3BD$ in THF. Spectroscopic inspection of the product by ^1H NMR, however, shows the typical quartet resonance of the hydride ligand of **4**. The intensity of this resonance (relative to those of Cp and PMe_3) corresponds, within experimental error, to that expected for **4**, indicating that there is little or no deuterium incorporation into the hydride position. The same result was obtained by carrying out the reaction in THF-d^8. Thus, the only possible source of the hydride ligand is another ligand of the precursor complex $CpMoCl(PMe_3)_3$. This result is fully consistent with the mechanistic interpretation of the decomposition of **1** (see *Discussion*).

(*F*) Computational studies

The gradient-corrected density functional (B3LYP) computational approach has been shown to be quite reliable for both geometries and energies.[35] Previous studies have shown that nonlocal DFT methods yield results within 5 kcal mol^{-1} of the experimental values.[36] Comparative studies of B3LYP and other computational approaches (DFT-BLYP and MP2 with various different basis sets) have been recently carried out on systems analogous to those reported here, where there is also a variability of spin state.[37,38] We are therefore confident that the computational approach chosen here provides us with significant results, especially in terms of trends.

Geometry optimizations have been carried out on both spin triplet and spin singlet $CpMoX(PH_3)_2$ and on spin singlet $CpMoX(PH_3)_3$ (X = H, Cl, OH, PH_2). Optimized geometrical parameters and total energies are collected in Table 1, while views of the optimized geometries and relative energy diagrams are shown in Fig. 3. All systems could in principle be calculated in two symmetric limiting forms, where the X ligand is either eclipsed with a Cp carbon atom (*e.g.*, **I**) or projecting onto the middle of a Cp C—C bond (staggered, **II**). Previous detailed studies on $CpMCl_2(PH_3)$ systems (M = Cr, Mo)[37] have shown that the two structures differ in energy by

Table 1 B3LYP-optimized geometric parameters (distances in Å and angles in °) and energy (in Hartrees) for $CpMoX(PH_3)_n$ (X = H, Cl, OH, PH_2 ; n = 2, 3)

	X = H			X = Cl			X = OH			X = PH_2		
	n = 2			n = 2			n = 2			n = 2		
	S = 1	S = 0	n = 3	S = 1	S = 0	n = 3	S = 1	S = 0	n = 3	S = 1	S = 0	n = 3
Mo—CNT[a]	2.098	2.003	2.032	2.041	2.036	2.027	2.052	2.071	2.061	2.069	2.051	2.036
Mo—X	1.739	1.701	1.722	2.472	2.451	2.633	2.012	1.969	2.095	2.566	2.315	2.696
Mo—P	2.496	2.464	2.462	2.538	2.486	2.514	2.548	2.463	2.460	2.523	2.475	2.489
			2.489[b]			2.521[b]			2.544			2.476
									2.526[b]			2.493[b]
CNT—Mo—X	114.89	101.32	105.66	128.64	129.02	109.38	130.78	123.70	106.63	125.42	127.93	105.19
CNT—Mo—P	133.76	127.59	124.63	123.47	122.87	124.07	124.85	122.40	123.53	125.15	121.16	123.94
			116.68[b]			112.84[b]			126.65			121.23
									105.70[b]			113.16[b]
X—Mo—P	81.40	79.65	71.90	88.95	93.39	73.88	85.43	97.75	83.88	89.59	95.78	76.65
			137.66[b]			137.78[b]			68.47			76.36
									142.01[b]			141.63[b]
P—Mo—P	89.69	104.38	83.83	92.49	83.02	82.66	92.66	83.45	82.66	90.93	84.31	82.24
			107.63[b]			110.70[b]			82.76			82.56
									109.02[b]			113.89[b]
Mo—X—H							124.05	124.62	118.71	103.26	127.41	101.23
											134.50	102.64
Energy	−278.1412	−278.1383	−286.4484	−292.5739	−292.5605	−300.8531	−353.4096	−353.4060	−361.6866	−285.2534	−285.2657	−293.5471

[a] CNT = Cp ring centroid. [b] Phosphorous *trans* to X in the 18-electron structures.

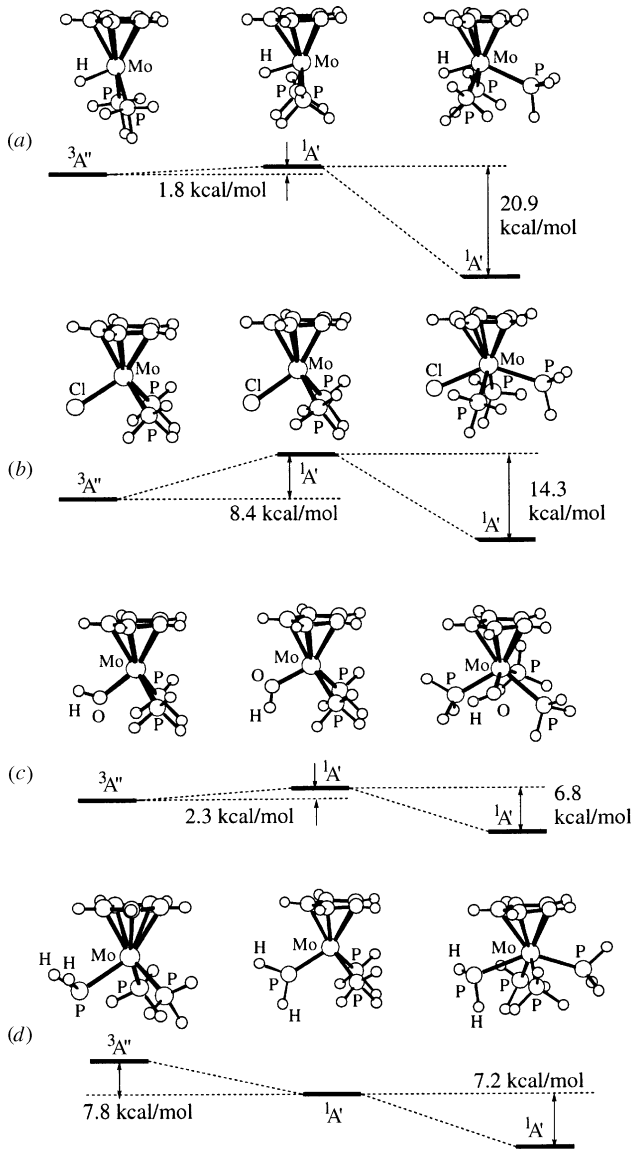

Fig. 3 B3LYP-optimized geometries and relative energies for the $CpMoX(PH_3)_2 + PH_3$ (left: singlet; center; triplet) and $CpMoX(PH_3)_3$ (right) systems. X = (*a*) H, (*b*) Cl, (*c*) OH, (*d*) PH_2. The B3LYP total energy of PH_3 is −8.269 867 hartrees

an insignificant amount. Both eclipsed and staggered calculations were carried out for the singlet and triplet $CpMo(PH_2)(PH_3)_2$ systems, confirming a negligible energy difference in both cases (0.2 kcal mol^{-1} in favor of **II** for the singlet, 0.3 kcal mol^{-1} in favor of **I** for the triplet). Therefore, all other calculations were arbitrarily carried out only with eclipsed Cp and X ligands.

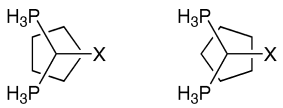

I **II**

All calculations on the H and Cl systems were carried out by imposing C_s symmetry. The 16-electron chloro system, $CpMoCl(PH_3)_2$, was previously examined at the MP2 level.[12] The B3LYP optimized parameters reported here are quite close to the corresponding MP2 parameters and to the experimental values. Since no structural model is available for the hydroxide system in either the 16-electron bis(phosphine) or the 18-electron tris(phosphine) configuration, a linear Mo—O—H starting configuration was arbitrarily chosen as the initial geometry for the hydroxide ligand in C_s symmetry. For the 16-electron systems, this evolved to a bent *endo* geometry (Mo—O—H angle = 124.05°) for the spin triplet structure and to a bent *exo* geometry (Mo—O—H angle = 124.62°) for the spin singlet structure. Both systems have also been calculated without any symmetry constraint and with a starting geometry having a Cp(center)–Mo—O—H dihedral angle of 90°, leading to a singlet local minimum [dihedral Cp(center)—Mo—O—H = 87.3°] 9.8 kcal mol^{-1} higher than the absolute minimum, or 12.1 kcal mol^{-1} higher than the triplet minimum [see Fig. 4(*a*)]. The metal–ligand distances are essentially identical with those of the absolute minimum. The major differences are observed for selected angle: the CNT—Mo—O angle has decreased substantially to 108.16°, and the Mo—O—H angle has decreased to 118.16°. This local minimum, therefore, is probably related to the existence of a barrier against rotation of the OH ligand around the Mo—O bond (see *Discussion*). The asymmetric spin triplet calculation, on the other hand, converged to the same geometry and energy as for the C_s system. The 18-electron $CpMo(OH)(PH_3)_3$ structure, meanwhile, was found to have a lower total energy with a bent asymmetric OH ligand [Cp(center)—Mo—O—H dihedral angle of 100.72°].

Analogously, no structural models are available for the phosphido compounds. Thus, the 16-electron PH_2 systems were calculated starting from various symmetric and asymmetric PH_2 conformations. The singlet geometry has lower energy when PH_2 is planar and perpendicular to the Cp ring (C_s symmetry), while the corresponding triplet prefers a pyramidalized arrangement, again C_s symmetric, with the H atoms bending toward the Cp ligand (*endo* conformation, see Fig. 3). The Mo—P—H and H—P—H bond angles in the triplet (103.26° and 95.01°, respectively) are indicative of a high contribution (>75%) of the phosphorus p orbitals in the bond hybrids and a smaller p contribution in the lone pair. The optimized 18-electron $CpMo(PH_2)(PH_3)_3$ model has an asymmetric, pyramidalized PH_2 group (sum of angles at P equal to 297°), with one P—H bond roughly parallel and another roughly perpendicular (*exo*) to the Cp plane.

Optimized metal–ligand distances are typically longer in the higher spin state for each 16-electron system, as has been found for other calculations[4] and attributed to differences in electron density distribution.[38] Addition of PH_3 causes the Mo—X distance to lengthen relative to the singlet state (by 0.021, 0.182, 0.126 and 0.381 Å for X = H, Cl, OH and PH_2, respectively). While the small lengthening of the Mo—H bond may be attributed to small σ effects caused by the introduction of the PH_3 ligand on the Mo—H bond, the much greater lengthening in the other cases is probably due to a combination of a σ effect and the rupture of the Mo—X π interaction (see *Discussion*). As for the Mo—PH_3 distances in the 18-electron systems, these are on the average greater in the order H < PH_2 < OH ≈ Cl, probably as a result of steric interactions (see *Discussion*).

The overall geometry of the 16-electron systems, with the notable exception of the hydride structures, is based on the "three-legged piano stool" in both spin states, *i.e.* on a pseudo-octahedral geometry with the Cp ring replacing three mutually facial ligands. In this geometry, the angles between bonds to two monodentate "leg" ligands should ideally be 90°, and the angles between any of these bonds and the CNT—Mo bond should be 125.26°. These angles are in the 83–97° and 122–131° ranges, respectively, for all systems (see Table 1) except for the $CpMoH(PH_3)_2$ systems, which can be better described as "four-legged piano stools" where the leg *trans* to the hydrido ligand is missing (see Fig. 3). The distortion is more pronounced for the singlet system. This dramatic difference is attributable to the small size of the hydrido ligand and to the lack of π interactions for the hydrido system (see *Discussion*).

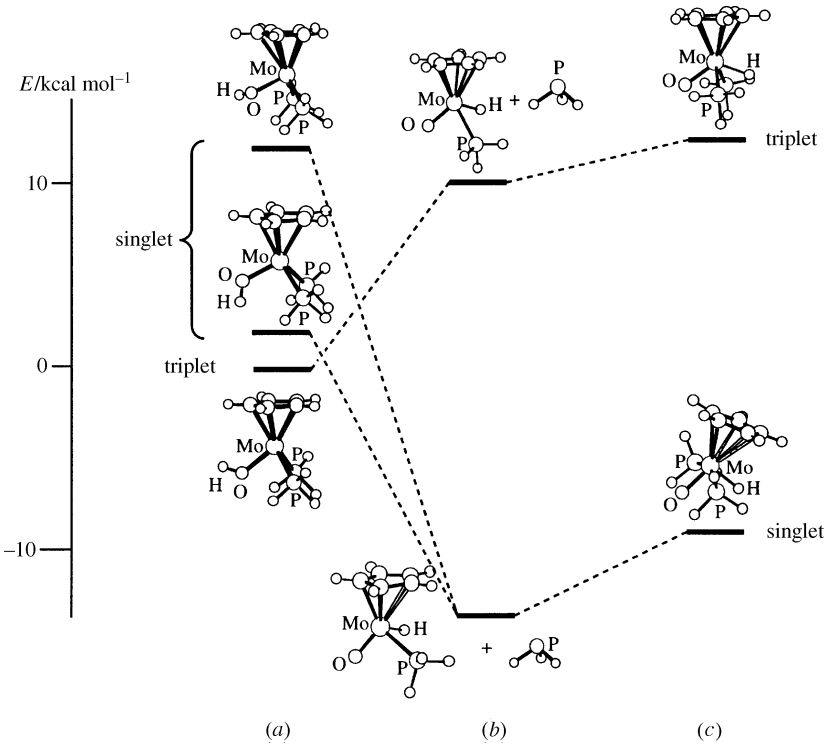

Fig. 4 B3LYP energies for singlet and triplet CpMo(OH)$(PH_3)_2$ (left), *trans*-CpMoH(O)$(PH_3)_2$ (center) and *cis*-CpMoH(O)$(PH_3)_2$ (right). A qualitative illustration of the optimized geometry is also given for each calculation. The dashed lines show correspondence between systems with the same spin state

The spin triplet geometry is calculated as more stable in all cases except for X = PH_2 (see Fig. 3), in full agreement with the available experimental findings. While compounds **1** and Cp*MoClL_2 (L = PMe_3 or L_2 = dppe)[20,21] have spin triplet ground states, Cp*Mo$(PPh_2)(PMe_3)_2$ is a stable diamagnetic compound.[19] Binding the PH_3 ligand to the spin singlet CpMoX$(PH_3)_2$, as is shown in Fig. 3, results in a stabilizing effect for all systems, the Mo—PH_3 binding energy relative to the singlet being in the order H > Cl > PH_2 > OH.

To further discount the possible alternative formulation of **1** as an oxo-hydrido derivative of Mo^{IV} rather than as a hydroxo derivative of Mo^{II} (*vide supra*), calculations were also carried out on singlet and triplet configurations for four-legged piano stool CpMoH(O)$(PH_3)_2$ geometries, with the PH_3 ligands both in *cis* and *trans* relative configurations. The results of these calculations are shown in Fig. 4. The calculations for the *cis*-CpMoH(O)$(PH_3)_2$ (no imposed symmetry) lead to the *expulsion of one PH_3 ligand* from the coordination sphere and the generation of a three-legged piano stool CpMoH(O)(PH_3), in both the singlet and the triplet spin state [Fig. 4(*b*)]. The triplet system has a high energy, + 10.0 kcal mol^{-1} relative to the triplet CpMo(OH)$(PH_3)_2$, while the singlet is stabilized by 13.8 kcal mol^{-1}. The Cp ring is distorted in both spin states with the carbon atom(s) opposite to the oxo ligand being farthest from the metal center. This feature can be attributed to the *trans* labilizing effect of the oxo ligand and is also experimentally observed by X-ray crystallography for the isoelectronic complexes $[CpMo(O)(PMe_3)_2]^+$ and Cp*ReOCl_2.[33,39] To the best of our knowledge, no stable complex having the CpMoH(O)(PR_3) stoichiometry has been reported to date. The isoelectronic $[CpMo(O)(PMe_3)_2]^+$ complex[22,24] has been shown to resist coordination of a third PMe_3 ligand.[33]

The *trans* geometry [Fig. 4(*c*)] was calculated with imposed C_s symmetry with the unique Cp carbon eclipsed with either the oxo or the hydrido ligand. Only the lowest energy structure is shown for each spin system. The triplet converged to a regular four-legged piano stool structure with a high energy value, 12.4 kcal mol^{-1} higher than spin triplet CpMo(OH)$(PH_3)_2$. The singlet configuration afforded a system with a severely distorted Cp ring at a higher energy relative to the singlet CpMoH(O)(PH_3) plus PH_3 system [see Fig. 4(*c*)].

Given that the oxo-hydrido Mo^{IV} formulations lead (as expected from the ability of the oxo ligand as a $\sigma + 2\pi$ donor) to strong preferences for singlet structures, the calculations provide further support to the assignment of the hydroxo Mo^{II} formulation to the paramagnetic compound **1**. The lack of a spontaneous transformation of **1** into a diamagnetic oxo-hydrido Mo^{IV} derivative with loss of PMe_3 will be addressed in the *Discussion* section.

Discussion

(*A*) Stability of the 16-electron spin triplet structure of 1

The calculations on the CpMoX$(PH_3)_n$ systems (X = H, Cl, OH, PH_2) were carried out with two objectives in mind, namely to understand which factors determine the choice of spin state for the 16-electron CpMoX$(PMe_3)_2$ structure and which factors determine the relative stability of these unsaturated complexes with respect to ligand adducts. In principle, steric effects, the participation of ligand lone pairs and a spin state change could contribute to the relative energetic stabilization of the 16-electron species relative to a ligand adduct. A separation of these factors is impossible from the experimental point of view. In addition, assessment of a metal–ligand π bond strength (even for systems where there are no spin state complications) is subject to experimental difficulties.[1] A kinetic approach was examined by Bryndza *et al.* for the PMe_3 dissociative exchange in Cp*RuX$(PMe_3)_2$,[40] but separation of the steric and electronic factors could not be achieved. We examine the spin state problem in this section and the M—PH_3 bond strength in the one that follows.

It is known from experiment that the 16-electron CpMoCl$(PR_3)_2$ and Cp* analogues have a spin triplet ground state,[20,21] and we now find the same preference for the

hydroxo derivative **1**. On the other hand, the isoelectronic phosphido complex $Cp^*Mo(PPh_2)(PMe_3)_2$ is diamagnetic.[19] The results of the B3LYP calculations on the $CpMoX(PH_3)_2$ (X = Cl, OH, PH_2) model compounds (see Fig. 3) are in perfect accord with the experiment. The choice between two spin states always depends, in monoelectronic terms, on two factors: a pairing energy and an orbital gap.[4] The nature of X influences the pairing energy by virtue of changes in Mo—X bond polarity, with the more electronegative ligands resulting in an increase of pairing energy *via* contraction of the metal orbitals. This effect was shown to determine the choice of spin state in the *trans*-$TiX_2(dmpe)_2$ (X = Cl, CH_3) systems[41] and $CpM(NO)X_2$ (M = Cr, Mo; X = Cl, CH_3).[38c] On the other hand, X can also have a profound effect on the orbital gap. As qualitatively discussed previously,[20] the two metal-based orbitals of interest are nonbonding relative to the Mo—X σ interaction, but they can both establish Mo—X π interactions if X has lone pairs with a suitable orientation.

The H ligand cannot establish any π interaction and the DFT calculations for this hydrido system show that the orbital gap (0.30 eV between the two semioccupied orbitals in the triplet state) is smaller than the pairing energy, giving a marginal preference to the triplet state. The major contribution to the lower-energy orbital is from the Mo d_{xy} orbital, while the higher-energy orbital is mostly Mo d_{z^2}, the *z* axis coinciding with the Mo—Cp(center) vector. This picture corresponds to the MO analysis of $CpML_4$-type complexes, first reported by Hoffmann and co-workers.[42] The Cl ligand is a double-faced π donor. Its lone pairs can interact with both HOMO and LUMO. The metal electrons will occupy the dπ–pπ out-of-phase (antibonding) combinations, qualitatively shown in **III** and **IV**. To a first approximation, the chlorine lone pairs are equally good at transferring π-electron density to the metal in both spin states. In the singlet state, there is a positive two-electron donation to one metal orbital and a filled-filled repulsion with the other, while in the triplet state there are two individual two-center-three-electron interactions, totaling six electrons in two π-orbital interactions for both spin states. While the orbital gap is raised in the singlet state (2.01 eV, relative to 0.27 eV for the triplet), the lack of a large difference in π stabilization plays in favor of the triplet by virtue of a reduced electron pairing. The larger triplet–singlet gap for the Cl relative to the H system, therefore, should mostly be attributed to a pairing energy difference, given the expected greater effective positive charge on the metal for the chloride complex.

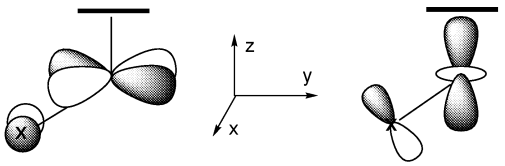

III **IV**

The variations of angular preference for the OH and PH_2 ligands in the spin triplet and singlet configurations (see Fig. 3) hint at the importance of Mo—X π effects for these two systems. For the hydroxo derivative, an important question is how many π interactions the OH lone pairs can establish with the Mo orbitals. The conventional view is that a linear (sp-hybridized) Mo—OH configuration allows the π interaction of both oxygen lone pairs, whereas for a bent geometry (approaching the sp^2 hybridization) the hybrid lone pair is rendered less available. However, the B3LYP optimization for the spin triplet $CpMo(OH)(PH_3)_2$ shows that the OH ligand establishes both π interactions in spite of a preferred bent geometry (*endo* conformation relative to the Cp ring), as shown in the qualitative interaction diagram of Fig. 5. This is rendered possible by the angular relationship between the

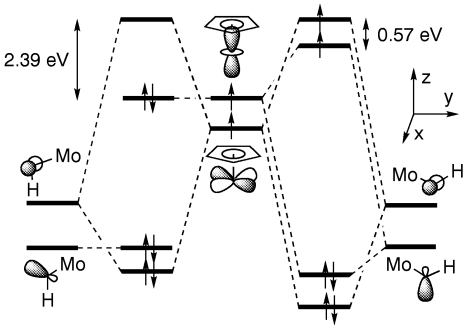

Fig. 5 Qualitative correlation diagram for the interaction between the Mo d_{z^2} and d_{xy} orbitals and the oxygen lone pairs in $CpMo(OH)(PH_3)_2$

metal d_{z^2} orbital and the Mo—O bond. For the *exo* singlet, on the other hand, the single two-electron π interaction occurs, as predictable, between the highest energy O lone pair (an essentially pure p orbital) and the lowest energy metal orbital (d_{xy}) to result in the observed *exo* configuration (see Fig. 5). The B3LYP calculation gives a 0.57 eV gap between the two singly occupied orbitals of the triplet and a 2.39 eV HOMO–LUMO gap for the singlet.

As attested by the similar optimized Mo—O distances in both spin states (see Table 1), the hydroxide ligand has a similar π donor strength in both spin states, formally providing two π electrons from one lone pair in the singlet and one π electron from each lone pair (in two distinct 2c–3e interactions) in the triplet. Thus, the OH system qualitatively behaves like the chloro system discussed above. However, the presence of the O—H bond in place of a Cl lone pair reduces the unfavorable filled-filled repulsion in the singlet state. Significantly, the bent *exo* OH ligand in the optimized singlet structure maximizes the distance between the O lone pair and the Mo d_{z^2} orbital. This rationalizes why the calculated triplet–singlet gap for the hydroxo system is smaller than for the Cl system, in spite of an expected greater pairing energy for the system with the more electronegative OH group. It is interesting to note that the singlet $CpMo(OH)(PH_3)_2$ local minimum for a parallel (relative to the Cp ring) Mo—O—H plane [Fig. 4(*a*)] is destabilized by 9.8 kcal mol^{-1} relative to the absolute singlet minimum. This destabilization can be attributed to a less favorable π donation from the higher energy oxygen p lone pair to the metal d_{z^2} orbital (*i.e.*, the in-phase combination corresponding to **IV**) and to a stronger OH(sp^2 hybrid)—Mo(d_{xy}) filled–filled repulsion.

The electronic situation drastically changes in the phosphido system, because the PH_2 ligand is a single-faced π donor. The singlet state involves only one profitable π interaction between the p lone pair of the perpendicular (relative to the Cp plane) PH_2 ligand and the metal d_{xy} orbital (see **III**) and no filled-filled repulsion, a situation analogous to that of the *exo* hydroxo complex. On the other hand, the triplet state can only benefit from a single 2c–3e interaction and, consequently, loses considerable π stabilization. Somewhat unexpectedly, the lowest energy optimized structure does not involve a π interaction with the energetically more favorable metal d_{xy} orbital, but rather with the d_{z^2} orbital, providing a pyramidalized $MoPH_2$ group with *endo* H atoms, similar to the *endo* triplet OH structure. It is likely that the choice of the metal d_{z^2} orbital for the π interaction is not dictated by the strength of the Mo—PH_2 three-electron π interaction, but rather by the greater stability of the pyramidalized P atom. Thus, when PH_2 can only donate one π electron (triplet state), the pyramidalization of P is the energetically dominating factor and the P lone pair (close to a sp^3 hybrid according to the bond angles) overlaps best with the energetically less favorable d_{z^2} metal orbital. Conversely, when PH_2 can donate

two π electrons (singlet state), the P—Mo π interaction becomes the energetically dominating factor and sacrifices the P pyramidalization. In this case, the P lone pair (p orbital) chooses the more favorable d_{xy} metal orbital. The PH_2 ligand has a low group electronegativity, thus a lower pairing energy could also contribute to the overall greater stability of the singlet state for $CpMo(PH_2)(PH_3)_2$.

In summary, the calculations show that the hydroxide ligand behaves, even though bent, as a double-faced π donor. This provides π stabilization and results in a low energy gap between the two highest energy metal-based orbitals. The latter feature, in combination with a high pairing energy, enforces the triplet ground state for compound **1**. A reduced filled-filled repulsion for the *exo* OH lone pair in the singlet, however, is responsible for a lower triplet–singlet gap relative to the chloro system.

(*B*) Energetics of the PMe_3 addition

It is known from experiment that $Cp^*Mo(PPh_2)(PMe_3)_2$ does not react with PMe_3, N_2 or CO,[19,43] whereas $Cp^*MoCl(PMe_3)_2$ reacts with all three, albeit quantitatively only with CO.[12,20] As we have shown here, **1** does not react with N_2 and PMe_3. However, it does bind CO to transform completely into a complex mixture of CO-, Cp- and PMe_3-containing products (see *Experimental*). Furthermore, our mechanistic interpretation of the decomposition of **1** (see below) indicates that the hypothetical $CpMoH(PMe_3)_2$ binds PMe_3 irreversibly. Thus, it appears that the binding ability of different $CpMoX(PMe_3)_2$ systems towards neutral two-electron donors goes qualitatively in the order $PR_2 < OH < Cl < H$. Steric factors definitely play an important role: while $CpMoCl(PMe_3)_3$ does not tend to dissociate any PMe_3, the 16-electron derivative is formed for some bulkier analogues *e.g.* $CpMoCl(PMe_2Ph)_3$ or $Cp^*MoCl(PMe_3)_3$.[21,23] On the other hand, all the trends observed along the $CpMoX(PMe_3)_3$ families cannot be fully characterized only with steric considerations. In fact, while Cl has a larger van der Waals radius than O (1.70–1.90 Å *vs.* 1.50 Å),[44] $CpMoCl(PMe_3)_3$ does not dissociate the third phosphine, while **1** does not coordinate PMe_3, even if the existence[22] of $[CpMo(OH)(PMe_3)_3]^+$ proves that there is sufficient room for coordination of a third PMe_3 ligand to **1**.

We have sought to understand to what extent various factors (steric and electronic in nature) regulate this different binding ability. For this purpose, we have chosen to compare all the different systems with respect to the PH_3 addition process [eq. (6)] in our computational studies. The results shown in Fig. 3 indicate a Mo—PH_3 strength in the order $H > PH_2 > Cl > OH$ relative to the ground state for each 16-electron system (triplet for H, Cl, OH; singlet for PH_2). It is to be considered that real systems may exhibit a slightly different ranking of strengths for steric reasons. Furthermore, the PH_3-binding process is necessarily accompanied by a decrease in entropy. However, the consideration of steric and entropic factors qualitatively reconciles the result of the calculations with the experimental results.

$$CpMoX(PH_3)_2 + PH_3 \rightleftharpoons CpMoX(PH_3)_3 \qquad (6)$$

We will now attempt to provide a more quantitative assessment of the factors regulating the strength of the Mo—PH_3 interaction in the different systems. The different bond dissociation energies (relative to the spin singlet 16-electron species) in Fig. 3 cannot be directly compared, because of differences in the geometries of the $CpMo(PH_3)_3$ and $CpMo(PH_3)_2$ fragments. These structural differences translate into differences in the steric strain upon PH_3 coordination, accompanied by other various electronic differences (*e.g.* orbital rehybridization). A way to correct for these differences is to calculate the energy differences between the radical "$CpMo(PH_3)_3$" and "$CpMo(PH_3)_2$" fragments at the fixed geometries found in the optimized $CpMoX(PH_3)_3$ and $CpMoX(PH_3)_2$ systems, respectively, and the total energy of the corresponding fully optimized (relaxed) fragment. These computed "relaxation energies" *E*(X) are 2.0 (H), 5.8 (PH_2), 9.3 (OH) and 12.8 (Cl) kcal mol^{-1} for the $CpMo(PH_3)_3$ fragment, and 1.0 (H), 5.7 (PH_2), 6.2 (Cl) and 6.5 (OH) kcal mol^{-1} for the $CpMo(PH_3)_2$ fragment (spin doublet derived from the optimized 16-electron singlets). These trends are roughly in agreement with differences in van der Waals size of the X group, Mo—X distance and on the lighter crowding in the bis(phosphine) system. The larger numbers for Cl relative to PH_2, especially for the tris-PH_3 system, may seem surprising. However, while the van der Waals sphere of Cl contains six electrons in one s and two p orbitals, that of PH_2 contains only two electrons in the P hybrid orbital. The optimized $CpMoX(PH_3)_3$ structures show that the PH_3 ligands are able to get closer to the X ligand and farther from each other when X is PH_2 relative to Cl. A greater steric effect of Cl relative to PH_2 is also evident from the optimized Mo—PH_3 distances (see *Results*). The Mo—PH_3 bond strengths relative to the 16-electron singlet state and corrected for steric effects are therefore 21.9 (H), 20.8 (Cl), 9.6 (OH) and 7.3 (PH_2) kcal mol^{-1}.

After the correction for steric effects, any difference in the Mo—PH_3 bond strength can only be attributed to electronic effects caused by modification of the ligand X. A first and obvious consideration is that the new Mo—PH_3 interaction necessitates a vacant metal orbital. All metal orbitals in 16-electron $CpMoX(PH_3)_2$ are engaged in M—X π interactions (*vide supra*), except for X = H. Part of the energy gained in the formation of the Mo—PH_3 bond is therefore spent in breaking the Mo—X π interaction. If this were the only factor at the source of the differences in Mo—PH_3 bond strengths, we could easily calculate the strength of the Mo—X bond in the singlet 16-electron compounds by normalization relative to the π-neutral hydride complex: X = Cl, 1.1; OH, 12.3; PH_2, 14.6 kcal mol^{-1}. These values are in agreement with the conventional view that hydroxide and phosphido ligands are better π donors than chloride. It has to be borne in mind, however, that there are also changes in the σ-bonding network beyond those taken into account within the "relaxation energy" correction factor, and perhaps also in the Mo—PH_3 π and Mo—Cp δ bonds, accompanying the coordination of the additional PH_3 ligand. Therefore, the above numbers can only be taken as indicative values. The most important σ effect is perhaps the *trans* influence of X on the newly formed Mo—PH_3 bond. We note, however, that the hydride is the strongest *trans*-labilizing ligand in the series examined here (*cf.* Mo—P_{trans} relative to Mo—P_{cis} bond lengths for each 18-electron compound in Table 1). Therefore, the effective π strength for the various Mo—X bonds may be greater than the numbers derived above. The order found for this system may not be valid in general, because a different trend was found for the Ru—NH_3 bond dissociation energy in $RuHX(CO)(PH_3)(NH_3)$ as a function of X.[45]

On the basis of all the computational results, it seems that the π stabilization is of paramount importance in providing a stable (*i.e.* isolable) 16-electron system with the $CpMoXL_2$ stoichiometry. The release of pairing energy on going from singlet to triplet state apparently provides only a secondary stabilizing factor: 16-electron systems can be stabilized and isolated with strong π donors in a singlet state [*e.g.* $Cp^*Mo(PPh_2)(PMe_3)_2$],[19] but there are as yet no known stable systems with a spin triplet configuration and π-neutral X ligands. However, the concept that a spin state change may help thermodynamically stabilize an unsaturated reaction intermediate,[4] thereby providing kinetic help to a reaction, appears justified.

In summary, the computational studies on the PH_3 addition process to $CpMo(OH)(PH_3)_2$ suggest that coordination of a third PMe_3 ligand to **1** is energetically discouraged by

two factors: the promotion to the singlet state and the disruption of the Mo—O π bonding, the latter being the most important factor. Analogous considerations can be applied to the hypothetical dimerization process to afford a di-μ-hydroxo structure, $[CpMo(\mu\text{-}OH)(PMe_3)_2]_2$, where each metal has achieved a saturated electronic configuration. An additional factor against dimerization is the filled-filled repulsion between the metal lone pairs. It is to be remarked that it is unusual to find hydroxide ligands in a terminal binding mode for organometallic compounds. The availability of lone pairs on the oxygen atom frequently leads to ligand loss and formation of doubly- or triply-bridged oligomers, such as for instance $Pt_2Cl_2(\mu\text{-}OH)_2L_2$ (L = tertiary phosphine),[46] $[Mo(CO)_2(NO)(\mu_3\text{-}OH)]_4$,[47,48] and $[Re(CO)_4(\mu_3\text{-}OH)]_4$.[49] Formally unsaturated organometallic compounds with terminal hydroxide ligands have rarely been observed for early and late transition metal systems, for instance $Cp^*_2M(OH)X$ (M = Zr, Hf; X = H, Cl, OH),[50] $Ir(OH)(CO)(PPh_3)_2$,[51] $M(CH_3)(OH)L_2$ (M = Pd,[52] Pt;[53–55] L = tertiary phosphine) and $Rh(OH)(CO)(PPr^i_3)_2$.[56] For molybdenum chemistry in particular, terminal hydroxide ligands are rare even when the metal is in a Werner-like coordination environment. To the best of our knowledge, the only two previous examples of formally 16-electron Mo^{II} complexes with terminal OH ligands are MoL(NO)(O)(OH) (L = 1,4,7-triisopropyl-1,4,7-triazacyclononane) and its corresponding protonated form, $[MoL(NO)(OH)_2]^+$.[57] These, however, do not contain M—C bonds and are diamagnetic, probably because extra π donation from the oxo lone pair(s) renders the compounds effectively saturated.

(*C*) Can α-H elimination from the hydroxo ligand occur?

The theoretical calculations on the PH_3 model system suggest that complex **1** is stabilized by Mo—O π bonding and by adopting a spin triplet ground state, but they also indicate that it could gain even greater stability by dissociating a phosphine ligand and undergoing an α-H elimination process from the OH ligand to afford a diamagnetic oxo-hydrido derivative of Mo^{IV} (see Fig. 4). There are precedents for the formation of stable oxo-hydrido compounds by α-H elimination from hydroxide ligands, *e.g.* $Cp^*_2Ta(O)H$.[58] This computational result has prompted us to investigate the thermal stability of **1**. As detailed in the *Results* section, no α-H elimination process occurs up to 70 °C, while decomposition takes place under more forcing conditions, but no diamagnetic hydride-containing products are observed. While it cannot be excluded that the decomposition occurs *via* initial α-H elimination from the OH ligand, the experimental observations clearly establish that the activation barrier for this process is high.

We observe that the process of α-H elimination from the OH ligand to afford the more stable (according to the calculation) oxo-hydrido product must involve, in whichever order, a 90° rotation of the OH ligand around the Mo—O bond, a reduction of the Mo—O—H angle leading to a Mo···H interaction and the α-elimination process, the dissociation of a PMe_3 ligand and a spin state change. The calculations show that rotation of the OH ligand involves loss of considerable stabilization (Fig. 4). In addition, it can be easily imagined that the transition state leading to the α-H elimination process and to the PH_3 dissociation requires additional energy. Even though a detailed analysis of hypothetical reaction coordinates was not carried out, the calculations on the PH_3 model systems suggest that a smooth, low-activation pathway for the α-H elimination process is not available.

(*D*) Mechanism of the decomposition of 1 in C_6D_6 and promotion of the PMe_3/C_6D_6 H/D exchange

The multitude of phenomena that are observed during the slow room temperature decomposition of **1** in C_6D_6 (see *Results*) raise a number of questions, all of which are satisfactorily answered, we believe, by the mechanism illustrated in Scheme 1. The decomposition is initiated by the oxidative addition of a solvent C—D bond. Deuterated benzene adds by far the fastest amongst all solvents tried, in agreement with trends established for the oxidative addition to other 16-electron intermediates.[59,60]

(*D*.1) Stoichiometry; formation of compounds 4 and 5. The formation of the hydride product **4** with PMe_3 incorporation implies transfer of the hydroxide oxygen atom to an acceptor molecule. This has been identified as the solvent C_6D_6, with formation of C_6D_5OH (see *Results*). It is to be observed that the direct conversion of a C—H bond to a C—OH bond (*e.g.* methane to methanol) is a topic of considerable current interest. A way to accomplish the observed transformation of C_6D_6 to C_6D_5OH is, as indicated in Scheme 1, oxidative addition of C_6D_6 to the 16-electron compound **1** (k_1) followed by reductive elimination of C_6D_5OH (k_3) to generate a 16-electron deuterido intermediate $CpMoD(PMe_3)_2$, **II**-D. Trapping of this intermediate by the available free PMe_3 would generate a stable 18-electron deuterido product, $CpMoD(PMe_3)_3$ (**4**-D). However, the decomposition leads to a majority of the hydride product **4**. This indicates that incorporation of the deuterido ligand into a coordinated PMe_3 ligand is faster than PMe_3 addition. This incorporation can easily be envisaged by the succession of PMe_3 *ortho*-metallation (oxidative addition, k_4^H), followed by the reverse reductive elimination process (k_{-4}^D) with ultimate exchange of a ligand H atom with the D atom and formation of another 16-electron intermediate, $CpMoH(PMe_3)(PMe_3\text{-}d^1)$, **II**-$d^{0,1}$ [we shall adopt a $d^{n,m}$ notation for compounds having the $(PMe_3\text{-}d^n)(PMe_3\text{-}d^m)$ isotopic substitution pattern]. Trapping of this intermediate by the free phosphine should lead to **4**-$d^{0,1}$, which cannot be distinguished from **4** by ^1H or ^{31}P NMR. However, subsequent PMe_3 exchange leads to free PMe_3-d^1, which is directly observed by ^{31}P NMR (see next section).

Formation of the other Mo-containing product of the decomposition, **5**, can be readily rationalized by the alternative reductive elimination of HOD from intermediate **I** (k_2). The reductive elimination of hydroxo and hydrido ligands to afford water does not appear to have a clear literature precedent. It was discounted for the thermolysis process of $Cp^*_2W(OH)H$[61] and for the water loss from $Cp^*_2Ta(^{18}OD)(^{16}OD)H$.[62] However, the reverse oxidative addition reaction of a water O—H bond is precedented, for instance for the complexes $[Rh(en)_2]^+$ and $[Ir(PMe_3)_4]^+$.[63–65] The latter affords *cis*-$[IrH(OH)(PMe_3)_4]^+$, which resists reductive elimination of water.[64] An alternative mechanism involving elimination of a hydroxide ligand followed by deprotonation does not appear likely in the apolar benzene solvent. The 16-electron pentadeuterophenyl derivative **IV** may subsequently evolve, as shown in Scheme 1, *via* the *ortho*-metallated intermediate **V**, analogous to **III**, which reductively eliminates C_6D_5H with ultimate formation of **5**. The same mechanism was previously proposed for the observed formation of **5** by reaction of $CpMoCl(PMe_3)_3$ with PhLi, presumably involving an unobserved $CpMo(C_6H_5)(PMe_3)_3$ intermediate.[23] There is, however, a second possible pathway for the generation of compound **5** [see section (*D*.4)].

(*D*.2) Promotion of H/D exchange. The first important fact to establish is that the observed free PMe_3-d^n isotopomers are not deriving from the *free* PMe_3-d^0 originally present in solution, but rather from the PMe_3 ligands of **1**. Therefore, this process is not a catalyzed H/D exchange between PMe_3 and C_6D_6 but rather a mere promotion of H/D exchange between

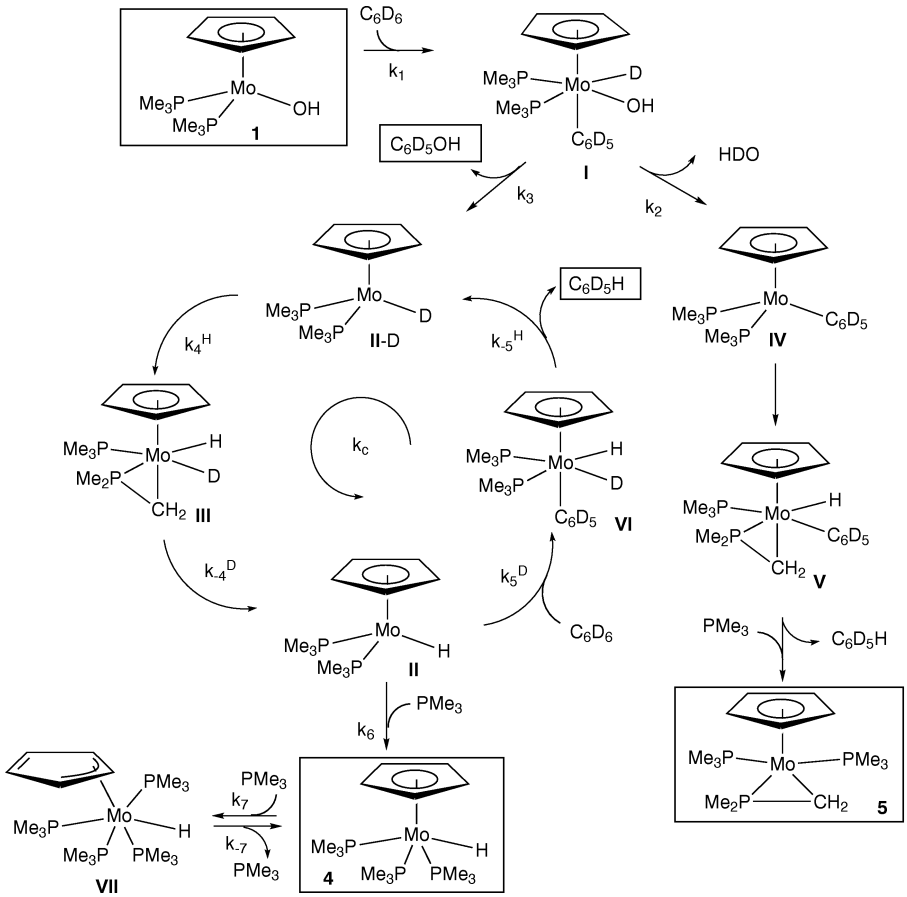

Scheme 1

the solvent and coordinated PMe_3. This is shown by the combination of two facts: (*i*) no PMe_3-d^n is formed from **1** in the presence of free PMe_3 *before* the formation of **4** (in fact, the release of free PMe_3-d^n is much slower than the conversion of **1** to **4**) and (*ii*) **4** is not a catalyst for the H/D exchange process: a genuine sample of **4** does not lead to the formation of any observable PMe_3-d^n ($n > 0$) over a period of several months upon standing in C_6D_6 in the presence of a small amount of free PMe_3. This observation also demonstrates that the trapping reaction of intermediate **II** in Scheme 1 to generate **4** must be irreversible. The irreversibility of this step is also indirectly suggested by another experiment: **4** does not react at room temperature with CO ($P = 1$ atm) over several days, whereas treatment of $CpMoCl(PMe_3)_3$ with CO results in the immediate replacement of one PMe_3 ligand to afford $CpMoCl(PMe_3)_2(CO)$, followed by further PMe_3/CO exchange. These observations are in agreement with the B3LYP calculated Mo—PH_3 bond strengths in $CpMoX(PH_3)_3$ (*vide supra*).

The formation of all possible PMe_3-d^n isotopomers indicates that the pathways of H/D exchange between a coordinated phosphine ligand and the C_6D_6 solvent must have the possibility of occurring repeatedly before the active species is trapped to afford **4**. Provision for this result is easily made by invoking an oxidative addition process of a C_6D_6 molecule at the level of the 16-electron intermediate **II**-d^{0,1} (k_5^D) to generate a Mo^{IV} hydrido-deuterido species **VI**-d^{0,1}, followed by reductive elimination of the observed C_6D_5H product (k_{-5}^H) to generate a deuteride intermediate **II**-D-d^{0,1}. By repeating the oxidative addition/reductive elimination process, the latter complex leads to either **II**-d^{0,2}, **II**-d^{1,1} or again **II**-d^{0,1}, depending on whether oxidative addition occurs at a C—H bond of either PMe_3 or PMe_3-d^1, or at the C—D bond of PMe_3-d^1. This cycle may be repeated a number of times with multiple incorporation of D atoms into the coordinated phosphine ligands. At each stage of the multiple H/D exchange cycle, competitive trapping of the 16-electron intermediates **II**-d^{n,m} and **II**-D-d^{n,m} by PMe_3 coordination (k_6) may also occur. It is important to consider that both intermediates **II** and **II**-D can equally undertake three different processes: (*i*) addition of free PMe_3, (*ii*) *ortho*-metallation of a PMe_3 ligand and (*iii*) oxidative addition of the C_6D_6 solvent. The rate constant for each of these processes should not strongly depend on whether the metal is bonded to a hydride or a deuteride ligand. On the other hand, while intramolecular oxidative addition of a phosphine C—H bond is productive when it occurs on intermediate **II**-D, the oxidative addition of C_6D_6 leads to a useful result only when it takes place on **II**.

While process (*i*) is irreversible (*vide supra*), processes (*ii*) and (*iii*) must necessarily be followed by the corresponding reverse process (either to return to the starting complex or to go forward to the H/D-exchanged complex). The greater amount of deuterium in the NMR solvent relative to hydrogen on the PMe_3 ligands statistically sets the thermodynamics in favor of the fully substituted PMe_3-d^9 product. Therefore, the observed distribution of the PMe_3-d^n products must be under kinetic control. We may define k_c as an effective turnover rate, intending for this the rate at which one ligand C—H bond (or a C—D bond already present) is replaced by a C—D bond. The value of k_c is not a simple function of the forward rate constants of the cycle but must also take into account the reversibility of all steps, which reduces k_c (and favors trapping of **II** by PMe_3 over continued H/D exchange). The rate with which **II**-d^{n,m} is trapped with formation of **4**-d^{n,m} is k_t ($= k_6[PMe_3\text{-d}^0]$).

The relative probability for **II**-d^{n,m} to either continue the H/D exchange process or be trapped is therefore given by the ratio k_c/k_t. More specifically, a fraction $x = k_t/(k_t + k_c)$ of molecules **II**-d^{n,m} exits the cycle, while the remaining fraction $(1 - x)$ will undertake an additional cycle. It is easy to predict

that if an extremely small fraction of **II** exited the cycle after each exchange event (very small x), the isotopic distribution would tend to favor the fully deuterated phosphine, PMe_3-d^9, as the sole product. On the other hand, if a large fraction of **II** exited the cycle, the distribution should be in favor of PMe_3-d^1. A qualitative examination of Fig. 2(*a*) indicates that the value of x must be small.

The irreversibility of process (*i*), together with the observed prevalent formation of **4**-$d^{n,m}$ over **4**-D-$d^{n,m}$, is an indication that the steady-state concentration of **II**-$d^{n,m}$ is greater than that of **II**-D-$d^{n,m}$ for each set of n and m values. Reductive elimination processes involving C—H(D) bonds are predicted to show a significant inverse isotope effect (that is, k_{-4}^{H}/k_{-4}^{D} and k_{-5}^{H}/k_{-5}^{D} should be significantly smaller than 1). Previously reported values of k^H/k^D, for instance, are 0.51(1) and 0.5(1) for the reductive elimination of RH from Cp*Rh(PMe_3)(R)(H) (R = 3,5-$C_6H_3Me_2$ and CH_2CH_3, respectively).[66,67] This fact alone can rationalize the greater steady-state concentration of **II** relative to **II**-D. In addition, there should be a direct kinetic isotope effect for the process of C—H oxidative addition (*i.e.* k_4 and k_5) to intermediates **II** and **II**-D. Previously reported k^H/k^D values for oxidative additions are slightly greater than 1, for instance 1.38 for the reaction of Cp*Ir(PMe_3) with C_6H_{12}/C_6D_{12}.[68] Thus, the *ortho*-metallation of a C—H bond to either **II** or **II**-D should be slightly favored over the *ortho*-metallation of a C—D bond to give steady-state concentrations of **III**-H_2 > **III**-HD > **III**-D_2. This would introduce an additional factor in favor of a greater steady-state concentration of **II** relative to **II**-D.

It is not possible to establish whether the resting state of the cycle is **III** or **VI** (in other words, whether the limiting rate for the cycle is k_{-4} or k_{-5}). This information could potentially be provided by the decomposition of **1** in C_6D_6 in the absence of free PMe_3. In principle, the most stable species within the H/D exchange cycle should be the observed final product under these conditions. However, **4** was still obtained in significant amounts, in addition to other Cp-containing products that do not exhibit any hydride resonances. This indicates that the resting state of the H/D exchange cycle is unstable relative to further decomposition involving loss of PMe_3, which then becomes available to trap intermediate **II**. The same Cp-containing by-products are also observed, albeit in much smaller relative amounts, during the decomposition of **1** in the presence of PMe_3.

Fig. 2 shows that the D-enriched PMe_3 ligands are eventually freed-up in solution. This process *cannot* take place by dissociation from **4**-$d^{n,m}$ because, as mentioned above, PMe_3 coordination to **II** is irreversible. The alternative is an associative exchange mechanism, which probably occurs *via* a slipped-ring intermediate **VII**. PMe_3-rich ring-slipped compounds are precedented in the literature.[69] A control study (see *Results*) has confirmed that PMe_3 exchange on compound **4** does take place (eq. 4).

It is also interesting to note that the presence of H_2 does not affect the course of the decomposition of **1** in C_6D_6 in the presence of PMe_3. In particular, there was no trace of the formation of the known compound $CpMoH_3(PMe_3)_2$,[23] which could be envisaged as the product of oxidative addition of H_2 to intermediate **II**. This means that intermediate **II** oxidatively adds the C—H(D) bonds of coordinated PMe_3 or the C—D bonds of the C_6D_6 solvent, or adds PMe_3, faster than it oxidatively adds H_2.

(*D*.3) Simulation of the deuterated phosphine distribution. The program implementation for the simulation, which aims to reproduce the PMe_3-d^n distribution in the early stages of the reaction, is based on the mechanism outlined in the previous section. The details of the program, along with the assumptions and approximations it relies on, are available from the authors. The optimized parameters are x, the fraction of molecules trapped after each H(D)/D exchange cycle, and the isotopic factor y, defined as k_4^H/k_4^D. The output of the simulation program for given values of the parameters x and y is a set of relative populations of the free PMe_3-d^n molecules, which is then plotted against the ^{31}P chemical shift and compared with the experimental spectrum. The process was repeated with different values for the parameters x and y until the best agreement between the experimental and the simulated spectra was obtained. The population distribution proved to be weakly sensitive to changes in the isotopic factor y; outputs obtained with y in the reasonable 1.1–1.5 range for the same value of x were very similar. Effects from changes of y, observable only when outrageous values for y were chosen (*e.g.* 4), showed that they were tantamount to changes of x at constant y. In light of these results, a value of $y = 1.3$ was arbitrarily imposed and only x was further optimized. The best simulated spectrum [Fig. 2(*c*)] was obtained for $x = 0.040$ (corresponding to $k_t/k_c = 0.042$). That is, 4.0% of intermediate **II** is trapped by PMe_3 after each H/D exchange cycle.

(*D*.4) Formation mechanism for the excess of PMe_3-d^1 from 1-OD. The observation of a significant difference in the isotopic distribution of free PMe_3-d^n from the decompositions of **1** and **1**-OD [*cf.* Fig. 2(*a*) and 2(*b*)], and notably the greater proportion of PMe_3-d^1 obtained from the decomposition of **1**-OD, can be rationalized by invoking an additional process that allows selective incorporation of the deuteroxide D atom into a PMe_3 ligand *before* the occurrence of the other processes examined in the previous sections. Given that, according to Scheme 1, competition before PMe_3 metallation and solvent oxidative addition may take place at the level of intermediates **II** and **IV**, a similar competition could be invoked at the level of compound **1**. Solvent addition (k_1) leads to the pathway previously discussed, whereas PMe_3 metallation (k_8, see Scheme 2) leads to a new intermediate (**VIII**), which is identical to intermediate **III** except for the presence of a deuteroxide ligand in place of a deuteride ligand.

Now, a mechanism must be found for interchanging the deuteroxide D atom and the hydride ligand in **VIII**. In principle, two pathways could render these two atoms equivalent: the first one is oxidative addition of the O—D bond to yield a Mo(H)(D)(O) moiety for an extremely unlikely 20-electron Mo^{VI} intermediate. The second, more likely, mechanism is reductive elimination of the hydrido and deuteroxide ligands to afford a Mo(OHD) moiety in the Mo^{II} intermediate **IX**. Reversal of this process by oxidatively adding the O—D bond, and subsequent reverse *ortho*-metallation, generates compound **1**-d^1, which can then reenter the H/D exchange cycle as discussed in the previous section. However, the PMe_3-d^n isotopic distribution would not be changed if *all* of the **1**-d^1 immediately entered the H/D exchange cycle at this point. A fraction of the PMe_3-d^1 ligand must be exchanged with the available free PMe_3-d^0 *before* complex **1** enters the cycle. A control experiment (eq. 5) confirms that the PMe_3 exchange process on complex **1** takes place relatively rapidly and it is logical to suppose that this process takes place *via* an associative mechanism in view of the computational results (*vide supra*). In excellent agreement with this proposed mechanism, treatment of **1** with an excess of PMe_3-d^9 generates not only free PMe_3-d^0 but also a significant amount of PMe_3-d^8 (and no other PMe_3-d^n with $1 \leqslant n \leqslant 7$!, see *Results*) *via* intermediates analogous to **VIII** and **IX**.

It is to be remarked that intermediate **IX** could also lead, *via* replacement of HDO or H_2O with PMe_3, directly to the observed product **5**. Experimental evidence that this process does take place is the formation of **5** (*and not* **4**!!!) during the slow decomposition of **1** in C_6D_{12}.

(*D*.5) Acceleration by protic substances. The last, perhaps most interesting observation on the decomposition of **1** that

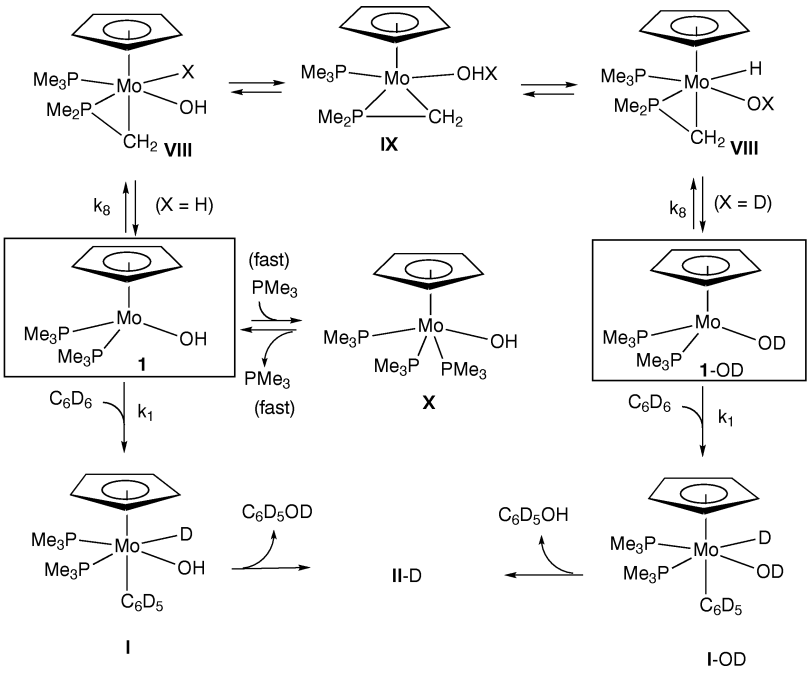

Scheme 2

needs to be rationalized is the catalytic effect of protic substances such as water and methanol. That this is a real catalysis is shown by the formation of identical decomposition products. The ratio between products **4** and **5** changes from 4 : 1 in the absence of catalyst to 10 : 1 in the presence of either water or methanol. This phenomenon could be rationalized by a reversibility of the HDO elimination step (k_2), but more detailed studies need to be carried out to further clarify this point. It is also important to notice that this catalytic effect is not related to the coordinating ability of water or methanol: no acceleration is observed in THF (in fact, the decomposition in neat THF is slower than in neat C_6D_6). As a corollary of the established catalytic effect, the formation of water during the decomposition of **1** (see Schemes 1 and 2) should make this reaction autocatalytic. The gathered qualitative experimental evidence (see *Results*) is consistent with this conclusion.

A relatively simple rationalization of this catalytic effect comes from an understanding of the electronic and molecular structure of **1**. We have learned that the 16-electron hydride intermediate **II**, as well as the deuteride analogue **II**-D, is extremely reactive and activates the C—H(D) bonds of the solvent or those of its own PMe_3 ligands at a much faster rate than the already favorable PMe_3 coordination. An oxidative addition process relies on the availability, at appropriate energies, of a metal-based empty orbital to accept the electrons of the bond being activated, plus a metal-based filled orbital to interact with the C—H(D) σ* orbital. This situation is realized in a spin singlet 16-electron fragment. Although the $CpMoH(PH_3)_2$ model is calculated to have a triplet ground state at the B3LYP level (*vide supra*), the triplet–singlet gap is within thermal energy and a spin-forbidden barrier is probably nonexistent.[4,15,70] A geometry reorganization-related barrier is also likely to be rather small, because the optimized singlet and triplet structures have very similar geometries (see *Results*). The same situation, on the other hand, is not realized for derivatives (of any electron count) where all the available metal orbitals heavily engage in π interactions with filled ligand orbitals. Such is the case for the spin singlet $Cp^*Mo(PPh_2)(PMe_3)_2$, where the single phosphido lone pair locks the only available metal orbital, or for the spin triplet $Cp^*MoCl(PMe_3)_2$, or for compound **1**. The X ligand lone pair(s) would have to be "pushed back" before the metal orbital could be used for any ligand addition or oxidative addition process.[1]

Since water and methanol share the property of having ionizable protons, and since the hydroxide lone pairs can easily engage in hydrogen bonding with sources of ionizable protons, it is relatively straightforward to imagine and propose that the action of water or methanol is simply to remove the OH lone pairs from the active π interaction with the metal orbitals and weaken or remove the HO—Mo π donation. Thus, the electronic structure of the complex, and consequently also its reactivity, would become similar to those of the hydride system and a C—H oxidative addition process may more easily take place.

In summary, the catalytic effect of water and methanol on the decomposition of **1** establishes an interesting new relationship between structure (molecular and electronic) and reactivity. To the best of our knowledge, the Brønsted acid-catalyzed activation of an unsaturated complex toward the oxidative addition of a C—H (or any other) bond had not been previously established.

(*E*) Mechanism of Cl/H metathesis in $CpMoCl(PMe_3)_3$

A final consideration of the reaction between $CpMoCl(PMe_3)_3$ and a hydride (or deuteride) reagent is appropriate. The molybdenum compound is quite electron-rich (as indicated by its low oxidation potential)[23] and is not likely to be attacked by nucleophilic reagents in an associative manner. The comparative reactivity of CO with $CpMoCl(PMe_3)_3$ (very fast) and $CpMoH(PMe_3)_3$ (**4**, too slow to be measured), in conjunction with the computational results reported in this contribution, indicate that dissociation of PMe_3 to afford a spin triplet 16-electron $CpMoX(PMe_3)_2$ intermediate is likely the necessary step for these reactions. Thus, by analogous considerations, the Cl/H (or Cl/D) metathesis reaction probably occurs *via* attack of the hydride (or deuteride) reagent on the 16-electron $CpMoCl(PMe_3)_2$. After the Cl/H (or Cl/D) exchange has occurred to afford intermediate **II** or **II**-D, PMe_3 adds again to afford the final 18-electron tris-phosphine product. As already established in section (*D*), however, intermediate **II**-D has sufficient time to exchange the deuteride ligand with a hydrogen atom of the PMe_3 ligand and give the more favored **II** (Scheme 3). There-

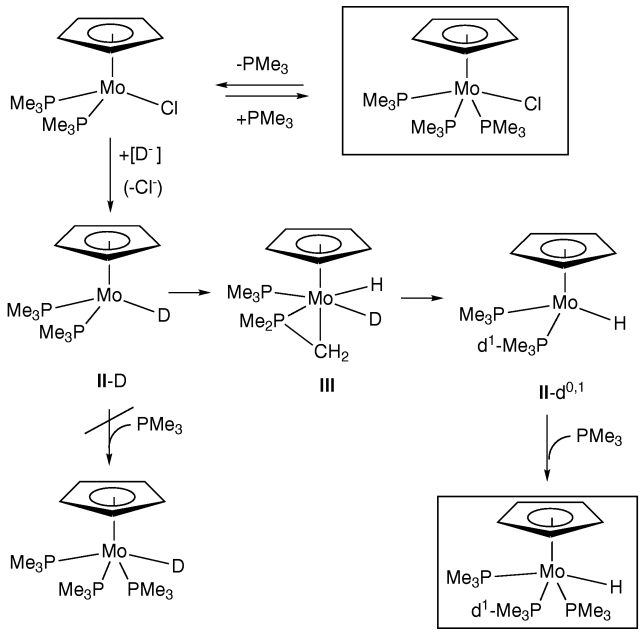

Scheme 3

fore, the formation of **4** (and not **4**-D) as the predominant product from $CpMoCl(PMe_3)_3$ and $LiEt_3BD$ fits well with the mechanistic proposal for the decomposition of **1** and with the results of the computational work.

Conclusion

We have examined in some detail the structure (both molecular and electronic)–reactivity relationship for the 16-electron $CpMoX(PMe_3)_2$ system and arrived at the following specific conclusions:

(*i*) When X is the electronegative and π donor hydroxide system, the compound is stabilized relative to products of dimerization, ligand additions or oxidative addition reactions by adoption of a spin triplet configuration and by the Mo—O π interactions, the latter being the most important factor.

(*ii*) Theoretical calculations on a model system with PH_3 ligands suggest that both oxygen lone pairs engage in π interactions, even for a bent Mo—O—H moiety. A reduced filled-filled repulsion in the *exo* singlet state determines the lower triplet–singlet gap relative to the Cl system.

(*iii*) An energetically favored (according to the calculations) α-H elimination with phosphine ligand dissociation to afford the Mo^{IV} system $CpMoH(O)(PMe_3)$ is kinetically inaccessible and is not experimentally observed.

(*iv*) When X, on the other hand, is the less electronegative and π-neutral hydride, the calculations on the 16-electron system yield a geometry that can promote facile ligand addition or oxidative addition processes. The induction of multiple H/D exchanges between the coordinated PMe_3 ligands and C_6D_6 during the decomposition of **1** is proposed to take place *via* the involvement of this very intermediate.

(*v*) The reactivity of the hydroxide complex is enhanced by proton sources that can establish hydrogen-bonding interactions with the OH lone pairs and thereby disrupt the Mo—O π interactions. The metal orbital that is freed up in this manner becomes available for C—H (or D) oxidative addition chemistry. There is, we believe, no previous example of the promotion of C—H activation by Brønsted acids *via* the diversion of stabilizing M—X π interactions into hydrogen bonding interactions.

In more general terms, we have examined in some detail the relationship between molecular structure, electronic structures and reactivity for a class of open-shell compounds of formula $CpMoX(PMe_3)_2$ (X = H, Cl, OH, phosphido), including an estimate of the strength of the MO—X π interaction. The results obtained and the considerations made should be relevant to a greater number of open-shell systems that constitute intermediates of stoichiometric or catalytic reactions.

Acknowledgements

We are grateful to the NSF (grant CHE-9508521) and the DOE (grant DEFG059ER14230) for support of this work and to Prof. Odile Eisenstein (Montpellier, France) for helpful discussions.

References

1 K. G. Caulton, *New J. Chem.*, 1994, **18**, 25.
2 C. A. Tolman, *Chem. Rev.*, 1997, **77**, 313.
3 T. L. Brown and K. J. Lee, *Coord. Chem. Rev.*, 1993, **128**, 89.
4 R. Poli, *Chem. Rev.*, 1996, **96**, 2135.
5 R. Poli, B. E. Owens and R. G. Linck, *J. Am. Chem. Soc.*, 1992, **114**, 1302.
6 F. Abugideiri, D. W. Keogh, H.-B. Kraatz, R. Poli and W. Pearson, *J. Organomet. Chem.*, 1995, **488**, 29.
7 A. A. Cole, J. C. Fettinger, D. W. Keogh and R. Poli, *Inorg. Chim. Acta*, 1995, **240**, 355.
8 J. C. Fettinger, D. W. Keogh and R. Poli, *J. Am. Chem. Soc.*, 1996, **118**, 3617.
9 J. C. Fettinger, S. P. Mattamana, R. Poli and R. D. Rogers, *Organometallics*, 1996, **15**, 4211.
10 J. C. Fettinger, D. W. Keogh, H.-B. Kraatz and R. Poli, *Organometallics*, 1996, **15**, 5489.
11 I. Cacelli, D. W. Keogh, R. Poli and A. Rizzo, *New J. Chem.*, 1997, **21**, 133.
12 D. W. Keogh and R. Poli, *J. Am. Chem. Soc.*, 1997, **119**, 2516.
13 S. P. Mattamana and R. Poli, *Organometallics*, 1997, **16**, 2427.
14. D. W. Keogh and R. Poli, *J. Chem. Soc., Dalton Trans*, 1997, 3325.
15 R. Poli, *Acc. Chem. Res.*, 1997, **30**, 494.
16 M. L. H. Green, *J. Organomet. Chem.*, 1995, **500**, 127.
17 E. Gross, K. Jörg, K. Fiederling, A. Göttlein, W. Malisch and R. Boese, *Angew. Chem., Int. Ed. Engl.*, 1984, **23**, 738.
18 M. Luksza, S. Kimmer and W. Malisch, *Angew. Chem., Int. Ed. Engl.*, 1983, **22**, 416.
19 R. T. Baker, J. C. Calabrese, R. L. Harlow and I. D. Williams, *Organometallics*, 1993, **12**, 830.
20 F. Abugideiri, D. W. Keogh and R. Poli, *J. Chem. Soc., Chem. Commun.*, 1994, 2317.
21 F. Abugideiri, J. C. Fettinger, D. W. Keogh and R. Poli, *Organometallics*, 1996, **15**, 4407.
22 J. C. Fettinger, H.-B. Kraatz, R. Poli and E. A. Quadrelli, *Chem. Commun.*, 1997, 889.
23 F. Abugideiri, M. A. Kelland, R. Poli and A. L. Rheingold, *Organometallics*, 1992, **11**, 1303.
24 M. Brookhart, K. Cox, F. G. N. Cloke, J. C. Green, M. L. H. Green, P. M. Hare, J. Bashkin, A. E. Derome and P. D. Grebenik, *J. Chem. Soc., Dalton Trans.*, 1985, 423.
25 H. G. Alt and J. A. Schwärzle, *J. Organomet. Chem.*, 1978, **162**, 45.
26 M. J. Frisch, G. W. Trucks, H. B. Schlegel, P. M. W. Gill, B. G. Johnson, M. A. Robb, J. R. Cheeseman, T. A. Keith, G. A. Petersson, J. A. Montgomery, K. Raghavachari, M. A. Al-Laham, V. G. Zakrzewski, J. V. Ortiz, J. B. Foresman, J. Cioslowski, B. B. Stefanov, A. Nanayakkara, M. Challacombe, C. Y. Peng, P. Y. Ayala, W. Chen, M. W. Wong, J. L. Andres, E. S. Replogle, R. Gomperts, R. L. Martin, D. J. Fox, J. S. Binkley, D. J. Defrees, J. Baker, J. P. Stewart, M. Head-Gordon, C. Gonzales and J. A. Pople, *Gaussian 94* (Revision E.1), Gaussian Inc., Pittsburgh, PA, 1995.
27 A. D. Becke, *J. Chem. Phys.*, 1993, **98**, 5648.
28 T. H. Dunning, Jr. and P. J. Hay, in *Modern Theoretical Chemistry*, ed. H. F. Schaefer, III, Plenum Press, New York, 1976, pp. 1–28.
29 P. J. Hay and W. R. Wadt, *J. Chem. Phys.*, 1985, **82**, 270.
30 P. J. Hay and W. R. Wadt, *J. Chem. Phys.*, 1985, **82**, 299.
31 W. R. Wadt and P. J. Hay, *J. Chem. Phys.*, 1985, **82**, 284.
32 L.-S. Wang, J. C. Fettinger and R. Poli, *J. Am. Chem. Soc.*, 1997, **119**, 4453.
33 J. C. Fettinger, H.-B. Kraatz, R. Poli, E. A. Quadrelli and R. C. Torralba, in preparation.
34 D. Astruc, *Angew. Chem, Int. Ed. Engl.*, 1988, **27**, 643.
35 D. G. Musaev, R. D. J. Froese, M. Svensson and K. Morokuma, *J. Am. Chem. Soc.*, 1997, **119**, 367 and references therein.

36 L. Deng, P. Margl and T. Ziegler, *J. Am. Chem. Soc.*, 1997, **119**, 1094.
37 I. Cacelli, D. W. Keogh, R. Poli and A. Rizzo, *J. Phys. Chem. A*, 1997, **101**, 9801.
38 (*a*) P. E. M. Siegbahn, *J. Am. Chem. Soc.*, 1996, **118**, 1487; (*b*) R. Schmid, W. A. Herrmann and G. Frenking, *Organometallics*, 1997, **16**, 701; (*c*) P. Legzdins, W. S. McNeil, K. M. Smith and R. Poli, *Organometallics*, 1998, **17**, 615.
39 W. A. Herrmann, E. Herdtweck, M. Flöel, J. Kulpe, U. Küsthardt and J. Okuda, *Polyhedron*, 1987, **6**, 1165.
40 H. E. Bryndza, P. J. Domaille, R. A. Paciello and J. E. Bercaw, *Organometallics*, 1989, **8**, 379.
41 C. Q. Simpson II, M. B. Hall and M. F. Guest, *J. Am. Chem. Soc.*, 1991, **113**, 2898.
42 P. Kubácek, R. Hoffmann and Z. Havlas, *Organometallics*, 1982, **1**, 180.
43 D. W. Keogh and R. Poli, unpublished results.
44 J. E. Huheey, E. A. Keiter and R. L. Keiter, *Inorganic Chemistry, Principles of Structure and Reactivity*, Harper & Row, New York, 1993.
45 D. Huang, J. C. Huffman, J. C. Bollinger, O. Eisenstein and K. G. Caulton, *J. Am. Chem. Soc.*, 1997, **119**, 7398.
46 M. E. Falkley and A. Pidcock, *J. Chem. Soc., Dalton Trans.*, 1977, 1444.
47 V. Albano, P. Bellon, G. Cini and M. Manassero, *J. Chem. Soc., Chem. Commun.*, 1969, 1242.
48 U. Sartorelli, L. Garlaschelli, G. Ciani and G. Bonora, *Inorg. Chim. Acta*, 1971, **5**, 191.
49 M. Herberhold, G. Süß, J. Ellermann and H. Gäbelein, *Chem. Ber.*, 1978, **111**, 2931.
50 G. L. Hillhouse and J. E. Bercaw, *J. Am. Chem. Soc.*, 1984, **106**, 5472.
51 S. A. Al-Jibori, *J. Organomet. Chem.*, 1996, **506**, 119.
52 V. V. Grushin and H. Alper, *Organometallics*, 1996, **15**, 5242.
53 T. G. Appleton and M. A. Bennett, *Inorg. Chem.*, 1978, **17**, 738.
54 D. P. Arnold and M. A. Bennett, *J. Organomet. Chem.*, 1980, **199**, 119.
55 D. P. Arnold and M. A. Bennett, *Inorg. Chem.*, 1984, **23**, 2110.
56 O. Gevert, J. Wolf and H. Werner, *Organometallics*, 1996, **15**, 2806.
57 J. Böhmer, G. Haselhorst, K. Wieghardt and B. Nuber, *Angew. Chem., Int. Ed. Engl.*, 1994, **33**, 1473.
58 G. Parkin, A. van Asselt, D. J. Leahy, L. Whinnery, N. G. Hua, R. W. Quan, L. M. Henling, W. P. Schaefer, B. D. Santarsiero and J. E. Bercaw, *Inorg. Chem.*, 1992, **31**, 82.
59 R. H. Crabtree, *Chem. Rev.*, 1985, **85**, 245.
60 W. D. Jones and F. J. Feher, *Acc. Chem. Res.*, 1989, **22**, 91.
61 G. Parkin and J. E. Bercaw, *Organometallics*, 1989, **8**, 1172.
62 G. Parkin and J. E. Bercaw, *Polyhedron*, 1988, **7**, 2053.
63 R. D. Gillard, B. T. Heaton and D. H. Vaughan, *J. Chem. Soc.* (*A*), 1970, 3126.
64 D. Milstein, J. C. Calabrese and I. D. Williams, *J. Am. Chem. Soc.*, 1986, **108**, 6387.
65 R. C. Stevens, R. Bau, D. Milstein, O. Blum and T. F. Koetzle, *J. Chem. Soc., Dalton Trans.*, 1990, 1429.
66 W. D. Jones and F. J. Feher, *J. Am. Chem. Soc.*, 1986, **108**, 4818.
67 R. A. Periana and R. G. Bergman, *J. Am. Chem. Soc.*, 1986, **108**, 7332.
68 A. H. Janowicz and R. G. Bergman, *J. Am. Chem. Soc.*, 1983, **105**, 3929.
69 J. M. O'Connor and C. P. Casey, *Chem. Rev.*, 1987, **87**, 307.
70 J. L. Detrich, O. M. Reinaud, A. L. Rheingold and K. H. Theopold, *J. Am. Chem. Soc.*, 1995, **117**, 11745.

Received in Montpellier, France, 14*th November* 1997;
Paper 7/09187G